SOFR Term Structure Dynamics — Discontinuous Short Rates and Stochastic Volatility Forward Rates

Alan Brace[1], Karol Gellert[2] and Erik Schlögl[3,4,5]

[1]FMMA — Financial Mathematics, Modelling and Analysis
[2]University of Technology Sydney, Australia
[3]University of Technology Sydney, Australia — School of Mathematical and Physical Sciences.
Erik.Schlogl@uts.edu.au
[4]African Institute of Financial Markets and Risk Management (AIFMRM), University of Cape Town, South Africa
[5]Faculty of Science, Department of Statistics, University of Johannesburg, South Africa

August 25, 2023

Abstract

The Secured Overnight Funding Rate (SOFR) has become the main Risk–Free Rate benchmark in US dollars, thus interest rate term structure models need to be updated to reflect the key features exhibited by the dynamics of SOFR and the forward rates implied by SOFR futures. Historically, interest rate term structure modelling has been based on rates of substantially longer time to maturity than overnight, but with SOFR the overnight rate now is the primary market observable. This means that the empirical idiosyncrasies of the overnight rate cannot be ignored when constructing interest rate models in a SOFR–based world.

As a rate reflecting transactions in the Treasury overnight repurchase market, the dynamics of SOFR are closely linked to the dynamics of the Effective Federal Funds Rate (EFFR), which is the interest rate most directly impacted by US monetary policy target rate decisions. Therefore, these rates feature jumps at known times (Federal Open Market Committee meeting dates), and market expectations of these jumps are reflected in prices for futures written on these rates. On the other hand, forward rates implied by Fed Funds and SOFR futures continue to evolve diffusively. We find that incorporating these empirical features into an interest rate term structure model are key to accurately fitting short-term instruments, in particular futures on one–month compounded SOFR. Informed by this, we construct a tractable multifactor, stochastic volatility term structure model which incorporates these features. Calibrating to prices for options on SOFR futures, we achieve a reasonable fit to the market across available maturities and strikes in a single, consistent model. The model also provides novel insights into SOFR term rate behaviour (and implied volatilities) within the SOFR term rate accrual periods, as well as a credible model mechanism by which interest rate mean reversion arises from monetary policy.

† The authors thank Leif Andersen and an anonymous referee for helpful comments on a previous version of this paper. The usual disclaimers apply.

1 Introduction

As the Secured Overnight Funding Rate (SOFR) is now the key Risk–Free Rate (RFR) benchmark in US dollars, interest rate term structure models need to be updated to reflect this. Historically, interest rate term structure modelling has been based on rates of substantially longer time to maturity than overnight, either directly as in the LIBOR Market Model,[1] or indirectly, in the sense that even models based on the continuously compounded short rate (i.e., with instantaneous maturity)[2] are typically calibrated to term rates of longer maturities, with any regard to a market overnight rate at best an afterthought. However, with SOFR this situation is reversed: The overnight rate now is the primary market observable, and term rates (i.e., interest rates for longer maturities) will be less readily available and therefore must be inferred (for example from derivatives prices).

Thus the empirical idiosyncrasies of the overnight rate cannot be ignored when constructing interest rate term structure models in a SOFR–based world, and more than longer term rates, these idiosyncrasies are driven by monetary policy. Already by simple inspection one sees that models, in which the short rate evolves as a diffusion, can no longer be justified by empirical data. Instead, the primary driver of the short rate is the piecewise flat behaviour of the Federal Open Market Committee (FOMC) policy target rate. Concurrently, we observe that the forward rates associated with the policy target rate evolve in a more diffusive manner. A model which reconciles these two features is the main contribution of this paper.

The literature refers to jumps with deterministic jump times as *stochastic discontinuities*, see for example Kim and Wright (2014), Keller-Ressel, Schmidt and Wardenga (2018), Fontana, Grbac, Gümbel and Schmidt (2020). The nomenclature reflects the treatment of discontinuities as extensions to an existing continuous stochastic model. Our approach is distinctly different in that the discontinuity is the basis of our model for the short rate, while simultaneously the forward rates for maturities beyond the next scheduled jump evolve as a continuous stochastic process.

Specific to SOFR, Heitfield and Park (2019) model forward rates using a step function, assuming that rates remain constant for all dates between FOMC meetings. This is a static approach for the purposes of calibrating a piecewise flat term structure. Andersen and Bang (2020) provide a SOFR–inspired general "spike" model to enable the extension of derivative pricing models to spikes in the short rate. While spikes in SOFR have been frequently observed in the past, regulatory changes and measures by the Federal Reserve have seen this phenomenon disappear since early 2020, thus our focus is exclusively on short rate discontinuities at known times. Inspired by the transition to an overnight benchmark in the United Kingdom, Backwell and Hayes (2022) propose and estimate a pure jump multicurve[3] model for British pound (GBP) LIBOR (London Interbank Offer Rate) and SONIA (Sterling Overnight Index Average) overnight index swap (OIS) rates, coining the term "scheduled jumps" for jumps at known times. However, for scheduled jumps in their model, the state variables impact the next jump only, and all scheduled jumps in the short rate beyond the upcoming central bank meeting date have expectation zero. By not following this "pure jump" approach, the model proposed in the present paper does not have this restriction, and also can still be embedded in a standard Heath, Jarrow and Morton (1992) (HJM) framework. We use indicator functions in the instantaneous forward rate volatilities to obtain piecewise constant paths of the short rate, while maintaining diffusive dynamics of forward rates maturing beyond the next central bank meeting date. Each factor is endowed with its own stochastic volatility and mean

[1] See Miltersen, Sandmann and Sondermann (1997), Brace, Gatarek and Musiela (1997) and Musiela and Rutkowski (1997).

[2] Of these, Hull and White (1990) is the most prominent example.

[3] Backwell and Hayes (2022) explicitly take into account basis spreads between interest rate term structures referencing different payment frequencies, in a manner similar to Backwell, Macrina, Schlögl and Skovmand (2023). This is not necessary in our present paper, since we consider futures (and options on futures) referencing SOFR only.

reversion. One could label this a "Heston/Hull–White" dynamic. In the literature, "Heston/Hull–White" usually refers to Heston (1993) stochastic volatility equity models with an interest rate driven by a Hull and White (1990) model, see for example Grzelak, Oosterlie and Weeran (2008). In the present paper, we instead consider a Markovian (in a small number of state variables), exponential affine interest term structure term structure model, where the stochastic volatility follows a Heston–type dynamic, and which in the one–factor, deterministic volatility case collapses back to a Hull/White model.

Several papers focus on adapting existing models to SOFR without considering discontinuities. These include Mercurio (2018), who uses a deterministic SOFR–OIS spread with a short rate model for the OIS. Lyashenko and Mercurio (2019) propose an extension to the LIBOR Market Model to accommodate the in–arrears setting nature of term rates related to SOFR and overnight benchmark rates in general. Skov and Skovmand (2021) show that a three–factor Gaussian arbitrage–free Nelson/Siegel model is well suited for the SOFR futures market, but they do not include the time series of SOFR itself in their estimation.

The model presented in the present paper is motivated by the empirical behaviour of SOFR and SOFR forward rates implied from futures, and we conduct a cross–sectional calibration to both futures and options. The proposed model performs well in cross–sectional calibration due to having a sufficient amount of variables which control various aspects of model behaviour. This allows the model to be calibrated across different maturities, underlying futures accrual periods and option strikes. This flexibility in the context cross–sectional calibration is similar to prominent models deployed in practice: The SABR model, introduced in Hagan, Kumar, Lesniewski and Woodward (2002), can be calibrated to implied volatility convexity and skew across strikes, but generally requires a new calibration per option expiry (and swap/forward rate tenor). Short rate models, such as Hull and White (1990), are usually calibrated to only co-terminal swaptions chosen to match an underlying trade[4] and a singular strike per swaption. The lognormal LIBOR Market Model model (LMM) is well suited for simultaneously calibrating to at the money swaptions across expiries and tenors. Most comparable in terms of ability to calibrate across expiry, underlying tenor and strike are stochastic volatility extensions to the LMM, see for example Piterbarg (2015) or Karlsson, Pilz and Schlögl (2017).

We also present an analysis of the model–implied behaviour of options in the accrual period. Interest in this behaviour is mostly driven by the practicalities of adapting existing LIBOR–based modelling to SOFR and therefore requires casting option behaviour in the accrual period to the behaviour of the dynamics of partially set forward term rates. In this context, we find that under simplifying assumptions our model is consistent with Lyashenko and Mercurio (2019). However, the model presented in this paper handles the case of partially set forwards more naturally than that paper, and also provides more granular insight into the decay characteristics of implied volatility within the accrual period.

Additionally, the proposed model reveals a connection between forward rate empirical behaviour and short rate mean reversion. In the HJM framework, mean reversion is usually embedded *a priori* as a decay function of forward rate volatilities. We include both a decay function and a piecewise constant component[5] in the HJM volatility function. However, remarkably we find that the piecewise component derived directly from empirical data without any shape restrictions closely resembles the decay function associated with mean reversion. We discuss the implication from this result in Section 5.

The rest of the paper is organised as follows. Section 2 examines the empirical behaviour of SOFR and the effective Fed funds rate (EFFR), motivating the model proposed in this paper. Section 3 presents the model for discontinuous short rates with continuous forward rates, including stochastic volatility. In Section 4.1, the model is fitted to time series data of SOFR futures. The objective here is not to conduct a full econometric study. Rather, we demonstrate that modelling jumps at known times substantially improves upon traditional diffusive term structure models when applied to instruments referencing the

[4]For example call dates in a callable note.

[5]This is in order to achieve a piecewise constant forward rate structure corresponding to FOMC meeting dates.

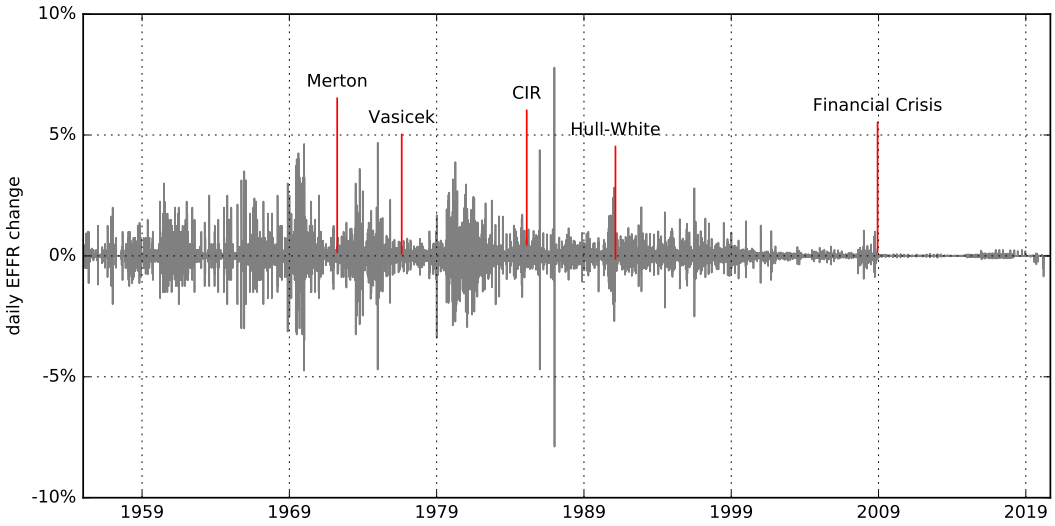

Figure 1: Empirical daily EFFR changes and the history of short rate models

new SOFR benchmark. The calibration of the stochastic volatility version of the model to cross–sectional prices for options on SOFR futures is presented in Section 4.2, showing that the proposed model is a viable alternative to existing models for the pricing and risk management of interest rate derivatives. Further implications of our model approach, on the in–accrual–period behaviour of implied volatility for options on one–month SOFR futures and on the connection between scheduled jump dynamics and mean reversion, are discussed in Section 5. Section 6 concludes.

2 Empirical Motivation

2.1 Monetary Policy and Short Rate Models

Over the course of the last five years, significant changes to the implementation of monetary policy have had a dramatic impact on the EFFR, resulting in a substantial divergence between its empirical behaviour and the dynamic assumptions of short rate models. The changes trace back to the 2008 financial crisis, prior to which monetary policy was administered primarily by direct intervention in the Fed Funds market to maintain the EFFR close to the target rate set by the FOMC. The approach relied on open market operations by the Federal Reserve trading desk resulting in the EFFR gravitating around the target rate with varying degrees of volatility.[6]

The first stochastic model of the short rate is attributed to Merton (1973), who employed a single–dimension Brownian motion as the driver. At least on cursory visual inspection, the empirical data at the time, see Figure 1, did not contradict the mathematically tractable Gaussian assumption of the model. The next major development came from Vasicek (1977), adding mean reversion, a strong empirical feature of rate dynamics. Modelling mean reversion also aligned with the notion of open market operations by the Federal Reserve trading desk managing the rate around the monetary policy target. Cox, Ingersoll and Ross (1985) (CIR) modified the dynamics of the continuously compounded short rate by scaling the volatility by the square root of the short rate, ensuring non-negativity of interest rates. The next milestone in short rate modelling was an extension of the Vasicek model with time dependent drift by Hull and White (1990), allowing the model to be fitted to an initial term structure of interest rates observed in

[6]See Hilton (2005) for an analysis of factors impacting EFFR volatility related to open market operations.

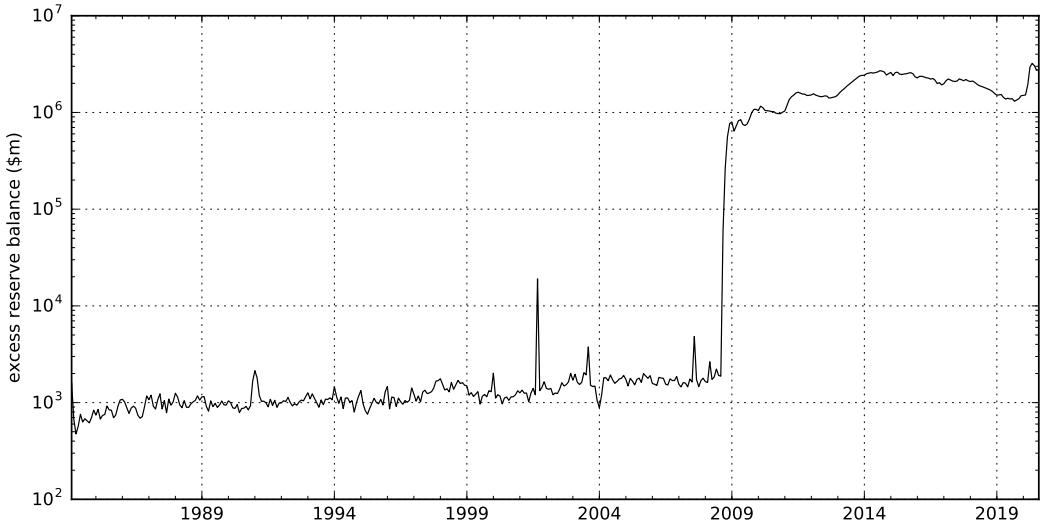

Figure 2: Excess reserves balance history

the market — this was critical for use of the model to price interest rate derivatives. Heath et al. (1992) developed the general framework into which all diffusion–based arbitrage–free interest rate term structure models must fit.

Open market operations are carried out by the Federal Reserve trading desk, whose trading goal is to maintain the EFFR near the target rate. This involves monitoring the market and counteracting trades which move the EFFR away from target, in essence micro–managing market liquidity. The 2008 financial crisis included a crisis in liquidity and the ability of the Federal Reserve's trading desk to maintain the EFFR near the target rate significantly deteriorated. The trading desk did not have the means to counteract the dramatic drain in supply of desperately demanded capital.

This was acknowledged by the Federal Reserve[7] as one of the factors considered when switching to a target range, initially set between 0 and 25 basis points. The Federal Reserve's strategy in response to the financial crisis centred around two key policies: near zero interest rates and quantitative easing. The phases of quantitative easing became known as QE 1/2/3 and involved selling Treasury bonds and purchases of various credit risky assets[8] in a bid to boost liquidity and improve credit conditions. The Federal Reserve's injection of liquidity resulted in an environment of elevated excess reserves. By historical standards, the rise in excess reserves was extreme and without precedent. As can seen in Figure 2, it increased from under $2 billion in September 2008 to $1 trillion by November 2009, before reaching a high of over $2.5 trillion in October 2015.

In October 2008, the Federal Reserve began paying IOER (interest on excess reserves)[9] to help control the EFFR in response to increasing excess reserves. It was thought at the time that the IOER should act as a lower bound for the EFFR, since no institutions should want to lend below this rate. As such, effective from October 9 the IOER was set to 75 basis points, with the EFFR target rate at 150 basis points. In the following days the EFFR was setting well below the target rate, including some days below the IOER. On the October 23, to lift rates closer to target, IOER was increased to 110 basis points, in response EFFR rates increased but were still setting below the IOER. Other adjustments were made in November under the assumption of IOER acting as a lower bound, however with EFFR persisting to

[7] See Federal Open Market Committee (2000-2020) December 2008, page 9.
[8] Such as Agency Debt, Mortgage Backed Securities and Term Auction Facilities, see Binder (2010).
[9] See Federal Open Market Committee (2000-2020) October 2008, page 7.

settle well below the IOER it became clear the assumption was incorrect.

In the FOMC immediately following the introduction of the IOER, it was noted that institutions not eligible to receive it were willing to sell (lend) funds at rates below the IOER.[10] However, it was not until December 2008, where together with the introduction of the target range, the IOER was set at the target range upper limit of 25 basis points in recognition that due to unique circumstances the IOER was acting as an upper bound for the EFFR. The large surpluses in excess reserves eliminated demand for reserve loans. Instead the Fed Funds rate was driven by Government Sponsored Institutions who do not earn interest on reserve balances, lending their excess reserves at below the IOER to institutions who would then earn the difference between the Fed Funds rate and the IOER. In effect, by paying the IOER in a market flooded with liquidity, the Federal Reserve became the borrower, rather than the lender, of last resort.

Plans for reversal of the post financial crisis expansionary policy were formally laid out at the FOMC September 2014 meeting as the Policy Normalization Principles and Plans.[11] The aim of the normalisation strategy was to bring the EFFR back to normal levels and reduce the securities held by the Federal Reserve, thereby unwinding the excess reserves held by banks. Prior to the financial crisis, controlling the supply of reserves via open market operations was a key tool in controlling the Fed Funds rate. However, the Federal Reserve has adopted the view that with banks using reserves for liquidity more than prior to the crisis, it might be hard to predict demand for reserves and therefore open market operations would not be effective at precisely controlling the EFFR.[12] Instead, the new normal will constitute the Federal Reserve keeping excess reserves just large enough to remain on the flat part of the demand curve, a prerequisite condition for the use of the IOER to control the EFFR.

Thus the conditions in the Fed Funds market are dramatically different to when short rate models were first conceived. The flood of liquidity in excess reserves, by construction aimed at removing any supply–demand gradient, has removed most of the volatility from the short rate of interest, with changes in the short rate being mainly driven by changes in the IOER, leading to jumps at known times (the FOMC meeting dates). Forward rates implied by traded market instruments, however, continue to exhibit volatility, as the evolution of market expectations of FOMC actions is priced into forward–looking instruments such as Fed Fund futures.

2.2 Secured Overnight Funding Rate

Shortly following the well–publicised LIBOR manipulation scandals, the Financial Stability Board and Financial Stability Oversight Council highlighted one of the key problems related to the reference rate to be the decline in transactions underpinning LIBOR and the associated structural risks to the financial system.[13] As argued in Schrimpf and Sushko (2019), partly to blame for the decline in interbank term lending are the inflated excess reserves discussed in the previous section.[14] In response, the Federal Reserve convened the Alternative Reference Rates Committee (ARRC)[15] to explore alternative reference rates. In June 2017, the ARRC formally announced the Secured Overnight Financing Rate (SOFR) as the replacement for LIBOR. A key criterion for the choice was the large volume of transactions behind SOFR, translating to it being more representative of bank's funding costs and less susceptible to manipulation. The calculation of SOFR is based on overnight repo transactions, which in 2017 averaged around $700b

[10] See Federal Open Market Committee (2000-2020) October 2008, page 2.

[11] See Federal Open Market Committee (2000-2020) September 2014, page 3.

[12] See Federal Open Market Committee (2000-2020) November 2018, page 3.

[13] See The Alternative Reference Rates Committee (2018), page 1.

[14] This suggests an interesting causal link between the financial crisis, the Federal Reserve response and the emergence of SOFR by linking the decline in LIBOR transactions to excess reserves.

[15] See https://www.newyorkfed.org/arrc

Figure 3: SOFR and FOMC target rate history

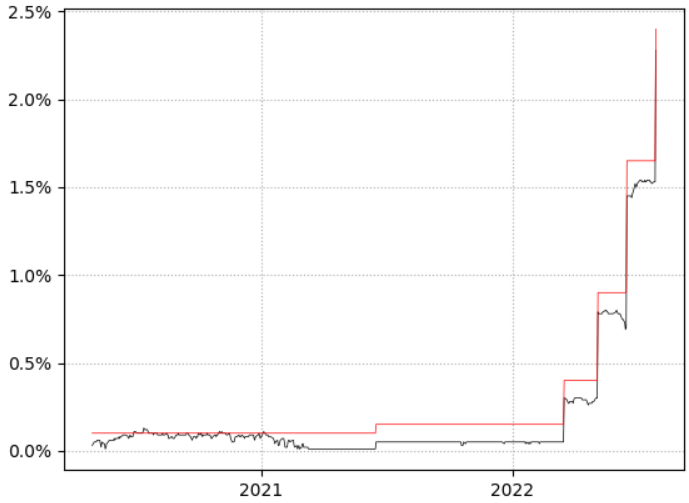

Figure 4: SOFR v FOMC target rate history May 2020 to August 2022

in daily transactions[16] (compared to less than $1b for US dollar LIBOR).

Official SOFR fixings have been calculated as far back 2014 and can be seen in comparison to the target rate in Figure 3. Three features stand out: To first order, SOFR appears to follow a stepwise function, suggesting that similarly to EFFR the Fed Funds target rate plays an important role in the SOFR dynamic. Another aspect is that SOFR is substantially more volatile than EFFR. A third feature is the prominence of spikes, most of which, similarly to EFFR, occur on the last trading day of the month. The end–of–month spikes are related to the measurement of dealers' balance sheet exposures at month–end for regulatory purposes. This single snapshot approach incentivises the management of exposures around reporting dates, which as explained in Schrimpf and Sushko (2019) has been resulting in increases

[16]For details see The Alternative Reference Rates Committee (2018), page 7.

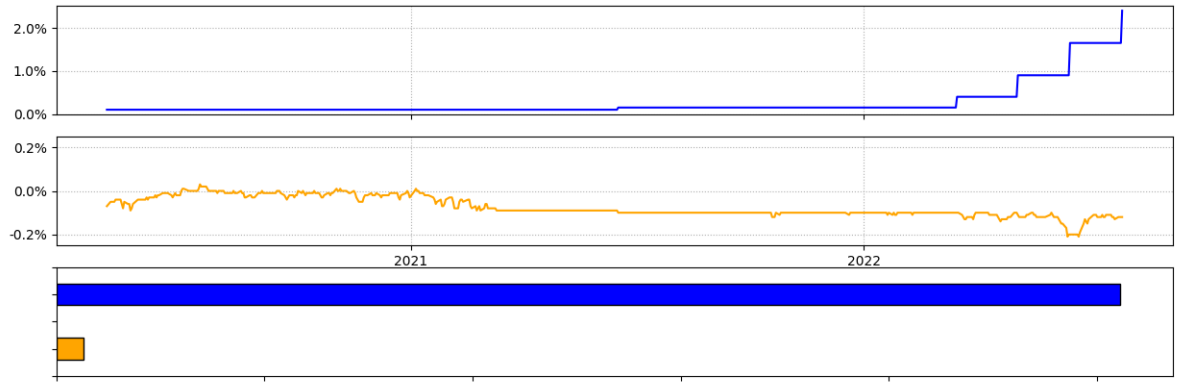

Figure 5: SOFR breakdown in vertical order (i) target rates (ii) SOFR-Target Rate spread (iii) variance contribution

in the SOFR rate on end–of–month dates. All three components historically contributed substantially to the observed daily variance of SOFR.[17] However, a very large spike in SOFR in September 2019 motivated the Federal Reserve to take action to effectively stabilise this rate. Since that time, as can be seen in Figure 4, spikes are no longer a feature of SOFR. The variance in SOFR is now dominated by changes in the policy target rate (around 99% of variance), with the remainder of the variance explained by a SOFR to target rate spread, see Figure 5. Consequently, the present paper focuses on modelling the policy target rate component.

2.3 Motivating stochastic volatility

Further motivation for the construction of our model are the empirical dynamics of the forward rate states, extracted from the data assuming term structure which are piecewise flat between FOMC dates, without any assumptions regarding the driving stochastic dynamics. Applying principal component analysis to obtain orthogonal factors, the time series of these factors clearly fail tests for normality. The quantile/quantile (QQ) plots in Figure 6 compare the expected quantile values for a normal distribution (red line) against the empirical value (blue dots). The dominant three PCA factors shown exhibit clear leptokurtosis, with excess kurtosis of 63, 10 and 2, respectively. Stochastic volatility is a common and parsimonious modelling choice to reproduce this feature.

One of the consequences of linking the model to FOMC dates is that some of the factor dynamics have a direct economic interpretation. As explained in Gellert and Schlögl (2021), the first factor focuses the dynamics on policy rate changes at the upcoming FOMC meeting, while the higher–order factors tend to focus on FOMC meetings beyond the next one. Excess kurtosis is notably highest for the first factor, suggesting a possible economic link between high leptokurtosis and the next FOMC meeting. This is in line with evidence from interest rate options, which imply a higher stochastic volatility for shorter expiry options. Anecdotally, interest rate market participants tend to focus on the next FOMC meeting date and the Federal Reserve tends to focus on managing the expectations related to the next FOMC date. This tends to make the expectations related to the next FOMC date most susceptible to news and changing economic circumstances, which offers a possible explanation of the excess kurtosis term structure.

[17] For a more detailed analysis, see Gellert and Schlögl (2021).

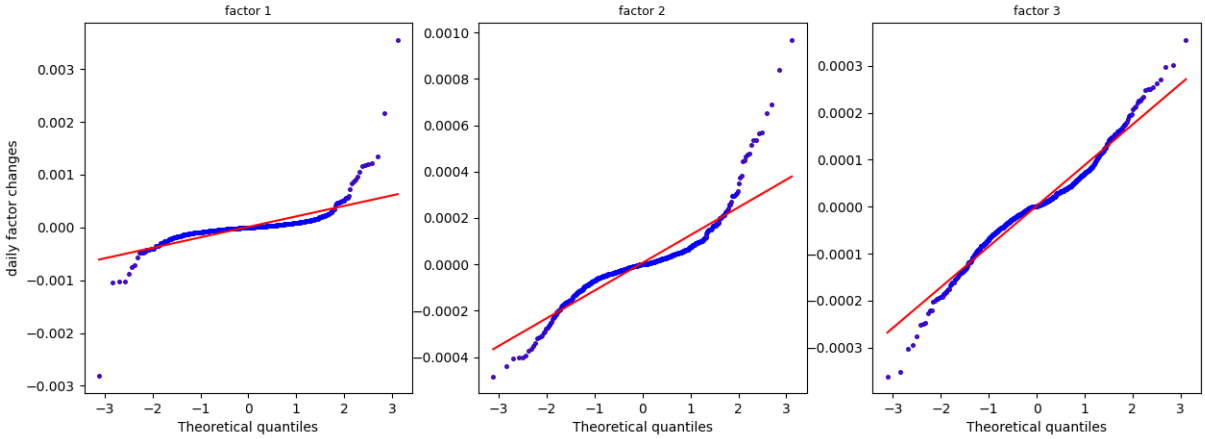

Figure 6: Empirical factor states quantile quantile plots

Another important aspect to consider is calibration to interest rate options. In general, calibration to interest rate options requires some freedom to fit the skewness and convexity of implied volatilities for a range of strikes. Interest rate options also tend to imply a term structure of volatility, skewness and convexity for a range of expiries and forward terms. Embedding stochastic volatility into each factor provides the ability to calibrate convexity and skewness[18] in addition to volatility level, with some control of the term structure of those features.

3 Modelling Short Rates with Discontinuities at Known Times

We have seen that the primary driver of EFFR and SOFR dynamics appears to be the changes in the Fed target, which is piecewise flat between the FOMC meeting dates at which a policy change has occurred. Most of the meetings are scheduled at least one year ahead of time with the exception of emergency meetings.[19]

Forward target rates do not trade directly, but the nature of their dynamics can be deduced from 30-day Fed Fund futures which trade on the closely related EFFR. Figure 7 shows the historical target rate and various forward rates implied from specific futures contracts. The point at which the forward rates end and meet the target rate coincides with the expiry of the futures contracts.[20] In contrast to the target rate, the dynamics of target forward rates are more diffusive and do not jump at deterministic dates. Jumps conceivably could occur on unexpected dates, reflecting sudden large changes in market sentiment, but in this paper we focus only on the diffusive aspect of forward rates. Furthermore, in the present paper we restrict ourselves to working with the policy (i.e., target) rate component only — this choice is supported by the results in the empirical analysis in Section 4 below.[21]

An interpretation of the forward rates deduced from futures is that they reflect the expectations of

[18] Skewness is impacted by the correlation of stochastic volatility to forward rate changes.

[19] Since 2015 there have been 61 meetings (including 3 emergency meetings), of which 21 resulted in a target rate change

[20] Futures without an FOMC date in the reference month were chosen such that the target rate is expected to be flat over the contract month and therefore the price of the futures reflects the expected target rate for that month plus a spread rather than reflecting two flat periods before and after the FOMC date.

[21] Obviously, the empirical fit could be improved further by modelling a stochastic spread between SOFR and the policy rate. However, this is not central to the present argument — see Gellert and Schlögl (2021) for such an extension to a different version of the model. That paper furthermore shows how to extend the model to cater for spikes in the short rate.

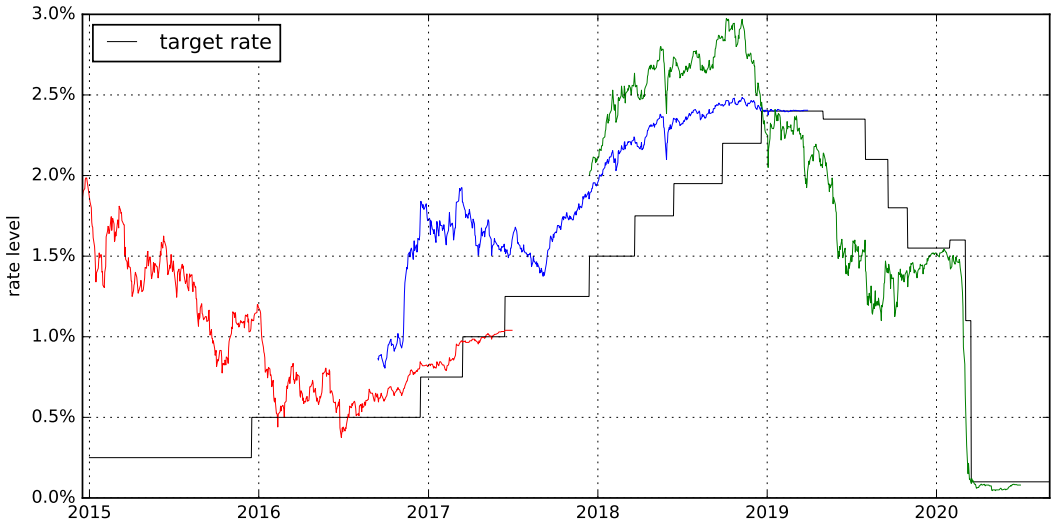

Figure 7: Target rate and various forward rates implied by specific 30–day Fed Funds futures

prospective FOMC target rate changes. The diffusive dynamics of forward rates then reflect the changes in those expectations. From this perspective, the expectations corresponding to each scheduled FOMC meeting are not independent of each other. In some circumstances, for example, a change in the overall Federal Reserve monetary policy stance, they will be positively correlated. In other cases, where for example the aggregated change to the target rate over some period of time is anticipated but the timing is less certain, the expectations may be negatively correlated to each other as the expected timing but not the net outcome evolves.

To recap, the target rate model is motivated by the following empirical features. The short rate $r(t)$ must be piecewise flat with respect to t. The forward rate with maturity T evolves diffusively with respect to t until the FOMC meeting immediately preceding maturity T, reflecting the expectations of any FOMC policy target rate change. We construct a model which reconciles these features, reflecting both the discontinuous nature of the short rate and diffusively evolving forward rates. The model is entirely driven by diffusions and can be cast directly in the Heath et al. (1992) (HJM) framework. While a diffusion process can be associated with the target rate change for each scheduled meeting date, in actual application these processes would be mapped to a smaller, more parsimonious number of factors by principal component analysis.

3.1 Reconciling piecewise constant short rates with diffusive forward rates

This modelling aim is achieved within the HJM framework by specifying instantaneous forward rate volatilities in terms of indicator functions based on the number of decision dates scheduled between the current ("calendar") time t and the forward rate maturity T. Starting point is the standard HJM result for forward rate dynamics with N factors under the spot risk–neutral measure:

$$f(t,T) = f(0,T) + \sum_{j=1}^{N} \int_0^t \sigma_j(u,T) \int_u^T \sigma_j(u,s) ds du + \sum_{j=1}^{N} \int_0^t \sigma_j(s,T) dW_j(s) \tag{1}$$

Define $\sigma_j(t,T)$ as a piecewise constant function between FOMC meeting dates:

$$\sigma_j(t,T) = \sigma_j \sum_{i=1}^{n} \gamma_{i,j} \mathbb{1}(i \leq \mathcal{A}_{t,T}) \tag{2}$$

where n is the total number of meetings dates and $\mathcal{A}_{t,T}$ reflects the number of meeting dates between t and T:

$$\mathcal{A}_{t,T} := \big|\{x_1, ..., x_m | t < x_i \leq T\}\big| \tag{3}$$

σ_j and $\gamma_{i,j}$ scale the volatility loading of each component of the driving (vector–valued) Brownian motion. σ_j allows control of the overall level of variance and is the key variable used in calibration to option prices. $\gamma_{i,j}$ scales the volatility based on the number of FOMC meeting dates between t and T. It can be empirically derived to reflect the covariance structure between forward rates. Solving the stochastic integral yields:

$$\begin{aligned} f(t,T) - f(0,T) = &\sum_{j=1}^{n}\sum_{q=1}^{n}\sum_{i=1}^{n} \sigma_j^2 \gamma_{q,j}\gamma_{i,j} \int_0^t \mathbb{1}(q \leq \mathcal{A}_{u,T}) \int_u^T \mathbb{1}(i \leq \mathcal{A}_{u,s}) ds du \\ &+ \sum_{j=1}^{n}\sum_{i=1}^{n} \sigma_j \gamma_{i,j} \mathbb{1}(i \leq \mathcal{A}_{0,T}) W_j(t \wedge x_{\bar{\imath}(T)}) \end{aligned} \tag{4}$$

where $\bar{\imath}(T) = \mathcal{A}_{0,T} - i + 1$. The solution reveals that the total variance is an increasing function of the number of meeting dates between 0 and T, up to the minimum of t and the last meeting date before T. This implies that the variance of the forward rate is zero if the forward date occurs prior to the next meeting date.

3.2 Introducing stochastic volatility

We introduce stochastic volatility into the model in a way that is inspired by what can be called a Heston/Hull–White (HHW) "quasi-Gaussian" model. This builds on the Gaussian Hull–White model by adding a Heston–type stochastic volatility component. Start with a one–factor quasi-Gaussian model (QG1) with the volatility function of instantaneous forward rates given by

$$\sigma(t,T) = \chi(t)\phi(T) \tag{5}$$

where $\chi(t)$ is generally stochastic. Under the spot risk–neutral measure we can write the dynamics of the instantaneous forward rates as

$$df(t,T) = F(t,T)dt + \sigma(t,T)dW(t) \text{ where } F(t,T) = \sigma(t,T) \int_t^T \sigma(t,u)du \tag{6}$$

$$\implies f(t,T) - f(0,T) = \int_0^t F(s,T)ds + \phi(T) \int_0^t \chi(s)dW(s) \tag{7}$$

Then set $T = t$ and differentiate with respect to t to express the spot rate $r(t)$ in the form

$$\begin{aligned} r(t) - f(0,t) = x(t) &= \int_0^t F(s,t)ds + \phi(t)\int_0^t \chi(s)dW(s), \quad x(0) = 0 \\ dx(t) &= \frac{d}{dt}\Big\{\int_0^t F(s,t)ds\Big\}dt + \phi'(t)\int_0^t \chi(s)dW(s) + \phi(t)\chi(t)dW(t) \\ &= \frac{d}{dt}\Big[\int_0^t F(s,t)ds\Big]dt + \frac{\phi'(t)}{\phi(t)}\Big[x(t) - \int_0^t F(s,t)ds\Big]dt + \sigma(t,t)dW(t) \end{aligned} \tag{8}$$

Define

$$\phi(T) = \exp\Big(-\int_0^T \lambda(v)dv\Big) \implies \frac{\phi'(t)}{\phi(t)} = -\lambda(t) \tag{9}$$

$$\chi(t) = \sigma(t)\exp\Big(\int_0^t \lambda(v)dv\Big) \implies \sigma(t,T) = \chi(t)\phi(T) = \sigma(t)\exp\Big(-\int_t^T \lambda(v)dv\Big) \tag{10}$$

therefore

$$F(t,T) = \sigma^2(t)\exp\Big(-\int_t^T \lambda(v)dv\Big)\int_t^T \exp\Big(-\int_t^u \lambda(v)dv\Big)du, \quad F(t,t) = 0 \tag{11}$$

Hence σ inherits the stochasticity of $\chi, \sigma(t,t) = \sigma(t)$ and the SDE changes to

$$dx(t) = \Big\{\frac{d}{dt}\Big[\int_0^t F(s,t)ds\Big] + \lambda(t)\int_0^t F(s,t)ds\Big\}dt - \lambda(t)x(t)dt + \sigma(t)dW(t) \tag{12}$$

in which the part of the drift term involving $F(t,T)$ simplifies to

$$\begin{aligned} \Phi(t) &= F(t,t) + \int_0^t \frac{\partial}{\partial T}F(s,T)\Big|_{T=t} ds + \lambda(t)\int_0^t F(s,t)ds \\ &= \int_0^t \sigma^2(s)\exp\Big(-2\int_s^t \lambda(v)dv\Big)ds = \int_0^t \sigma^2(s,t)ds \end{aligned} \tag{13}$$

The volatility $\sigma(.)$ is made stochastic by incorporating a Heston process $v(.)$ in it:

$$\sigma(t) \to \sigma(t)\sqrt{v(t)} \tag{14}$$

which results in an affine system of stochastic differential equations, which can be expressed under the spot risk–neutral measure as

$$\begin{aligned} dx(t) &= [\Phi(t) - \lambda(t)x(t)]dt + \sigma(t)\sqrt{v(t)}dW(t), \quad x(0) = 0 \\ d\Phi(t) &= [\sigma^2(t)v(t) - 2\lambda(t)\Phi(t)]dt, \quad \Phi(0) = 0 \\ dv(t) &= \theta(t)(1 - v(t))dt + \alpha(t)\sqrt{v(t)}dU(t), \quad v(0) = 1 \end{aligned} \tag{15}$$

with

$$\langle dW(.), dU(.)\rangle(t) = \rho dt \tag{16}$$

Bond price dynamics can be written as follows (see Appendix A for derivation):

$$B(t,T) = \exp\Big(- \int_t^T f(t,u)du \Big) = \frac{B(0,T)}{B(0,t)} \exp\Big(- \Lambda(t,T)y(t) - \frac{1}{2}\Phi(t)\Lambda^2(t,T) \Big) \tag{17}$$

where:

$$\Lambda(t,T) = \int_t^T \exp\Big(- \int_t^u \lambda(v)dv \Big) du \tag{18}$$

$$\Phi(t) = \int_0^t \sigma^2(s) \exp\Big(- 2\int_s^t \lambda(v)dv \Big) ds \tag{19}$$

3.3 Piecewise constant short rates with diffusive forward rates under stochastic volatility

Merging the modelling of Sections 3.1 and 3.2, assume now that each factor evolves with its own, independent Heston–type stochastic volatility. That is, each factor in the model of Section 3.1 is extended in the same manner as the single factor in Section 3.2. This model thus inherits the piecewise constant short rates with diffusive forward rates, but with stochastic volatility dynamics.

This set–up provides ample flexibility to calibrate to the volatility term structure (since each factor impacts different aspects of the forward rate term structure), as well as option–implied volatility skew and smile across different expiries. The level of flexibility is regulated by the number of factors and degree of time–dependence of the model parameters.

Starting point is again the standard HJM result for forward rate dynamics with N factors under the spot risk–neutral measure:

$$f(t,T) = f(0,T) + \sum_{j=1}^{N} \int_0^t \sigma_j(u,T) \int_u^T \sigma_j(u,s) ds du + \sum_{j=1}^{N} \int_0^t \sigma_j(s,T) dW_j(s) \tag{20}$$

We define the j-th component of the instantaneous forward rate volatility function as follows:

$$\sigma_j(t,T) = \sum_{i=1}^{n} \mathbb{I}_{\{i \leq \mathcal{A}(t,T)\}} \chi_j(t) \phi_j(T) \gamma_{i,j} \tag{21}$$

where

$$\phi_j(T) = \exp\Big(- \int_0^T \lambda_j(s) ds \Big) \tag{22}$$

and

$$\chi_j(t) = \sigma_j(t) \sqrt{v_j(t)} \exp\Big(\int_0^t \lambda_j(s) ds \Big) \tag{23}$$

$v(t)$ evolves with a Heston–type dynamic:

$$dv(t) = \theta(t)(1 - v(t))dt + \alpha(t)\sqrt{v(t)}dU(t), \quad v(0) = 1 \tag{24}$$

with

$$\langle dW_j(.), dU_j(.)\rangle(t) = \rho_j dt \tag{25}$$

and

$$\langle dW_i(.), dU_j(.)\rangle(t) = 0, \text{ for } i \neq j \tag{26}$$

The bond price dynamics for a single factor[22] can be written as (see Appendix A for derivation):

$$B(t,T) = \exp\Big(- \int_t^T f(t,u)du \Big) \tag{27}$$

$$\begin{aligned}
&= \frac{B(0,T)}{B(0,t)} \exp\Bigg(- \sum_{b=0}^{\eta(t)-2} \Lambda_{x_{\eta(T)-1}}(x_{b+1},T) y_{\eta(T)-1}(x_{b+1}) - \Lambda_{x_{\eta(T)-1}}(t,T) y_{\eta(T)-1}(t) \\
&- \sum_{k=\eta(t)}^{\eta(T)-2} \sum_{b=0}^{\eta(t)-2} \Lambda_{x_k}(x_{b+1},x_{k+1}) y_k(x_{b+1}) - \sum_{k=\eta(t)}^{\eta(T)-2} \Lambda_{x_k}(t,x_{k+1}) y_k(t) \\
&- \frac{1}{2} \sum_{b=0}^{\eta(t)-2} \sum_{i=1}^{\eta(T)-1-b} \sum_{j=1}^{\eta(T)-1-b} \gamma_i \gamma_j \Phi(x_b, x_{b+1}) \{\Lambda^2(x_{b+1},T) - \Lambda^2(x_{b+1}, x_{\eta(T)-1})\} \\
&- \frac{1}{2} \sum_{i=1}^{\eta(T)-\eta(t)} \sum_{j=1}^{\eta(T)-\eta(t)} \gamma_i \gamma_j \Phi(x_{\eta(t)-1}, t) \{\Lambda^2(t,T) - \Lambda^2(t, x_{\eta(T)-1})\} \\
&- \sum_{k=\eta(t)}^{\eta(T)-2} \frac{1}{2} \sum_{b=0}^{\eta(t)-2} \sum_{i=1}^{k-b} \sum_{j=1}^{k-b} \gamma_i \gamma_j \Phi(x_b, x_{b+1}) \{\Lambda^2(x_{b+1}, x_{k+1}) - \Lambda^2(x_{b+1}, x_k)\} \\
&- \sum_{k=\eta(t)}^{\eta(T)-2} \frac{1}{2} \sum_{i=1}^{(k-\eta(t)+1)} \sum_{j=1}^{(a-\eta(t)+1)} \gamma_i \gamma_j \Phi(x_{\eta(t)-1}, t) \{\Lambda^2(t, x_{k+1}) - \Lambda^2(t, x_k)\} \Bigg)
\end{aligned} \tag{28}$$

3.4 SOFR term rates

The transition of the key (US dollar) interest rate index from LIBOR to SOFR (with similar transitions for many other curencies) imposes on the market a change from benchmark rates set for a longer term (usually three months) to rates with an effective term of one business day. Transitioning to daily frequency for derivative instruments would not be desirable for many reasons, including burdening the system with a large increase in transaction volumes to settle daily flows. Instead, the market is adopting an approach where instruments are still defined with longer term rates, but those term rates are now calculated using either a compounding or averaging of SOFR over the term. This is what is typically called "term SOFR."[23]

[22] Since the model specification results in driving factors which are mutually independent, the generalisation of this expression to the multifactor case is straightforward, though notationally tedious.

[23] If one takes into account the "multicurve" phenomenon observed in interest rate markets, these "SOFR term rates" are more akin to rates implied by overnight index swaps (OIS) than actual term rates such as LIBOR, see Alfeus, Grasselli and Schlögl (2020) and Backwell et al. (2023). However, here we only consider instruments referencing SOFR, so this distinction is not needed in the present paper.

A LIBOR term would be defined by the start date T_i and an end date T_k of the period over which it applies. A SOFR term for the corresponding dates is defined as a set of discrete dates $\{T_i, , , T_k\}$ on which SOFR is observed. The most common definition of term SOFR is based on compounding over the term (usually 3m):

$$S(T_i, T_k) = \tau_{i,k}\left[\prod_{j=i}^{k}(1 + s(T_j)\delta_j) - 1\right] \tag{29}$$

where $\tau_{i,k}$ is the year fraction of the term length and $s(t)$ is the SOFR observed set for T_j. δ_j is the year fraction for the period between T_j and T_{j+1}, in order to account for days on which SOFR is not observed (weekends and holidays). For the empirical results presented in this paper, we make the assumption that the daily SOFR rate is approximated by the continuous short rate $r(t)$.

3.5 Pricing Futures

Define a 3M SOFR futures contract $F(T_i, T_k)$ with accrual period starting at T_i and ending at T_k, with payoff measurable at T_k:

$$F(T_i, T_k) = 100\Big(1 - S(T_i, T_k)\Big) \tag{30}$$

where $\delta_{i,k}$ is the year fraction between T_i and T_k. Using the generic futures pricing theorem,[24] the time t futures price $F(t, T_i, T_k)$ is given by the expected value at t under spot risk–neutral measure, i.e.

$$F(t, T_i, T_k) = E_\beta\Big[F(T_i, T_k)|\mathcal{F}_t\Big] \tag{31}$$

3.6 Pricing Options on Futures

Options on 3M SOFR futures exist for a variety of strikes and expiries. They are specified with American–style exercise, but we use them to approximate European–style implied volatilities, as is common in practice. We do not address the impact of the American exercise in this paper, instead we use these options to demonstrate the ability of the model to calibrate to a variety of strikes and expiries. The value of a call option at time t, expiring at $T_e < T_i$ with strike K, on the futures contract, can be expressed as the expected discounted payoff under the spot risk–neutral measure:

$$C(t, T_e, F(T_i, T_k), K) = E_\beta\left[\frac{1}{\beta(T_e)}(F(T_i, T_k) - K)^+|\mathcal{F}_t\right] \tag{32}$$

3.7 Simulating the model

As an initial proof of concept, particularly the ability of the model to calibrate to options on SOFR futures, we price options by Monte Carlo simulation.[25] For the stochastic integral component in Equation (20), we have:

$$\int_0^t \sigma_j(s, T)dW_j(s) = \sum_{i=1}^{n} \mathbb{I}_{\{i \le \mathcal{A}(t,T)\}}\gamma_{i,j}\phi_j(T)\int_0^t \sigma_j(s)\sqrt{v_j(s)}\exp\left(\int_0^s \lambda_j(q)dq\right)dW_j(s) \tag{33}$$

[24] See Cox, Ingersoll and Ross (1981).

[25] The HHW stochastic volatility dynamics assumed in our model would permit the derivation of semi-analytical option pricing formulae using Fourier transform techniques, but we leave such derivations to future work.

Setting constant parameters $\sigma_j(s) = \sigma_j$ and $\lambda_j(q) = \lambda_j$:

$$\int_0^t \sigma_j(s)\sqrt{v_j(s)}\exp\left(\int_0^s \lambda_j(q)dq\right)dW_j(s) = \sigma_j \int_0^t \sqrt{v_j(s)}e^{s\lambda_j}dW_j(s) \tag{34}$$

The stochastic component is approximated as follows:

$$\int_0^t \sqrt{v_j(s)}e^{s\lambda_j}dW_j(s) \approx \frac{1}{N}\sum_{p=1}^{N} g(t) \tag{35}$$

where

$$g_j(t) = \int_0^t \sqrt{v_j(s)}e^{s\lambda_j}dW_j(s) \tag{36}$$

calculated with Euler discretisation:

$$\Delta g_j(s) = \sqrt{v_j(s)}e^{s\lambda_j}\Delta W_j(s) \tag{37}$$

where $\Delta W_j(s) \sim N(0, \sqrt{\Delta t})$, $v_j(s) = v_j(s - \Delta t) + \Delta v_j(s)$ and:

$$\Delta v_j(s) = \theta(1 - v_j(s - \Delta t))\Delta t + \alpha\sqrt{v_j(s - \Delta t)}\Delta U_j(s), v_j(0) = 1 \tag{38}$$

where $\Delta U_j(s) \sim N(0, \sqrt{\Delta t})$ and $\langle \Delta W_j(.), \Delta U_j(.)\rangle(s) = \rho_j \Delta t$

4 Applying the Model to Market Data

4.1 Comparison to a traditional diffusive model

Firstly, we seek to demonstrate the impact of modelling scheduled jumps on the quality of fit to time series data, taking as a reference point the results of Skov and Skovmand (2021), who consider a three–factor Gaussian arbitrage–free model based on Nelson/Siegel–type[26] term structures. They estimate their model on data for one–month and quarterly SOFR futures, and we will use these same instruments. The period of observation also aligns with Skov and Skovmand (2021), beginning in June 2018 to capture the first full month of trading, through to June 2021, thus consisting of 757 trading dates.

To sharpen the focus on the "scheduled jump" aspect of our model (and to make it more comparable to Skov and Skovmand (2021)), we consider a version of our model without stochastic volatility.

4.1.1 Fitting the Gaussian version of the model to data

Define the observation period as a set of discrete dates $(t_0, ..., t_n)$, corresponding to trading days for SOFR futures. On each of the dates we observe a set of SOFR futures settlement prices consisting of 1m and 3m futures, denoted as $F_j^1(t_a)$ and $F_j^3(t_a)$ respectively. The subscript j indicates the position of the contract maturity, e.g. $F_3^1(t_a)$ is the third maturing 1m contract from t_a.

[26] See Nelson and Siegel (1987).

Denote the corresponding model price as $\hat{F}_j^1(t)$ and $\hat{F}_j^3(t)$. Using the generic futures pricing theorem, under the spot risk neutral measure we have:

$$\hat{F}_j^1(t_a) = E_\beta\left[\hat{F}_j^1(\tau_j^1(t_a))\big|\mathcal{F}_{t_a}\right] = 100 - \frac{100}{D_j^1(t_a)}\left[S_j^1(t_a) + G_j^1(t_a)\right] \tag{39}$$

where $\tau_j^1(t_a)$ is the terminal date and $D_j^1(t_a)$ is the number of calendar dates in the reference period of the contract. $S_j^1(t_a)$ accounts for the accrued SOFR fixings if the contract is trading during the reference period:

$$S_j^1(t_a) = \sum_{i=n_j^1(t_a)}^{(t_a^*-1)\wedge N_j^1(t_a)} r(t_i)d_i \tag{40}$$

where t_a^* is the index of time t_a, $n_j^1(t_a)$ is the index of the first date in the reference period and $N_j^1(t_a)$ is the index of the last date in the reference period. d_i is the number of calendar days to which the rate at time t_i applies, in order to allow for accrual over non-trading dates. The upper limit for the sum reflects that SOFR is published the day following its reference date. $G_j^1(t_a)$ represents the sum of the SOFR forward rates relevant to the reference period:

$$G_j^1(t_a) = E_\beta\left[G_j^1(\tau_j^1(t_a))\big|\mathcal{F}_{t_a}\right] = \sum_{i=t_a^*\vee n_j^1(t_a)}^{N_j^1(t_a)} E_\beta\left[r(t_i)\big|\mathcal{F}_{t_a}\right]d_i \tag{41}$$

where

$$E_\beta\left[r(t_i)\big|\mathcal{F}_{t_a}\right] = E_\beta\Bigg[f(t_a,t_k) + \sum_{j=1}^{n}\int_{t_a}^{t_k}\sigma_j^P(u,t)\int_u^{t_k}\sigma_j^P(u,s)dsdu + \sum_{j=1}^{n}\int_{t_a}^{t_k}\sigma_j^P(s,t_k)dW_j^P(s)\Bigg|\mathcal{F}_{t_a}\Bigg] \tag{42}$$

$$= f(t_a,t_k) + \sum_{j=1}^{n}\int_{t_a}^{t_k}\sigma_j^P(u,t)\int_u^{t_k}\sigma_j^P(u,s)dsdu \tag{43}$$

The price of the quarterly SOFR futures is based on the compounding payoff defined for the contract:

$$\hat{F}_j^3(t_a) = 100 - 100\left[\mathcal{S}_j^3(t_a)\mathcal{G}_j^3(t_a) - 1\right]\frac{360}{D_j^3(t_a)} \tag{44}$$

$\mathcal{S}_j^3(t_a)$ accounts for the compounded SOFR fixings if the contract is trading during the reference period:

$$\mathcal{S}_j^3(t_a) = \prod_{i=n_j^3(t_a)}^{(t_a^*-1)\wedge N_j^3(t_a)}\left(1 + \frac{r(t_i)d_i}{360}\right) \tag{45}$$

$\mathcal{G}_j^3(t_a)$ represents the compounding of the SOFR forward rates relevant to the reference period. Strictly speaking, we have

$$\mathcal{G}_j^3(t_a) = E_\beta \left[\prod_{i=t_a^* \vee n_j^3(t_a)}^{N_j^3(t_a)} \left(1 + r(t_i)\frac{d_i}{360}\right) \middle| \mathcal{F}_{t_a} \right] \tag{46}$$

However, we make two approximations, which greatly simplify calculations, but turn out to have insubstantial numerical impact. Firstly, we set

$$\mathcal{G}_j^3(t_a) \approx \prod_{i=t_a^* \vee n_j^3(t_a)}^{N_j^3(t_a)} \left(1 + E_\beta\Big[r(t_i)\big|\mathcal{F}_{t_a}\Big]\frac{d_i}{360}\right) \tag{47}$$

Furthermore, we ignore the convexity correction due to the distinction between expectations under the spot and forward measures, and set

$$E_\beta\Big[r(t_i)\big|\mathcal{F}_{t_a}\Big] \approx f(t_a, t_i) \tag{48}$$

In Appendix B, we compare the "calibrated prices" of the futures contracts used in our analysis, i.e., the prices calculated under the above approximating assumptions using the empirically fitted model parameters, with the corresponding prices calculated without making these assumptions (using Monte Carlo simulation). As Table 3 shows, the impact of the approximations (47) and (48) is negligible.

For each day in the observation period, assume forward rates are piecewise constant between FOMC dates and solve:

$$\boldsymbol{f}(t_a) = \underset{\boldsymbol{f}(t_a)}{\arg\min}\, O(t_a) \tag{49}$$

where $\boldsymbol{f}(t_a)$ is the vector of forward rates $f(t_a, t_i)$ which are piecewise constant between FOMC dates. The objective function is defined as the sum of squared errors between the price given $\boldsymbol{f}(t_a)$ and the market price for monthly and quarterly futures:

$$O(t_a) = \sum_j (\hat{F}_j^1(t_a) - F_j^1(t_a))^2 + \sum_j (\hat{F}_j^3(t_a) - F_j^3(t_a))^2 \tag{50}$$

The vector $\boldsymbol{f}(t_a)$ can instead be expressed as a step function:

$$f(t_a, T) = f_0(t_a) + \sum_{i=1}^{n} v_i(t_a)\mathbb{1}(i \leq \mathcal{A}_{t_a,T}) \tag{51}$$

from which we can extract a vector of discrete forward rate levels $(f_0(t_a), ..., f_n(t_a))$, where:

$$f_k(t_a) = f_0(t_a) + \sum_{i=1}^{k} v_i(t_a) \tag{52}$$

Changes in v_i correspond to changes in FOMC policy rate change expectations. To obtain the empirical dynamics, we need to extract the changes in v_i. For any dates t_a not immediately following an FOMC meeting:

$$\Delta v_i(t_a) = v_i(t_a) - v_i(t_{a-1}), t_{a-1} \notin \{x_0, ..., x_n\} \tag{53}$$

For dates following an FOMC meeting we need to consider the effect of rolling the FOMC meeting index:

$$\Delta v_i(t_a) = v_i(t_a) - v_{i+1}(t_{a-1}), t_{a-1} \in \{x_0, ..., x_n\} \tag{54}$$

v_{n+1} is by definition not observed, therefore we truncate the estimate to $n-1$ FOMC dates. Define a matrix of $\Delta v_i(t_a)$ observations.

$$\boldsymbol{V} = \begin{bmatrix} \Delta v_1(t_1) & \dots & \Delta v_{n-1}(t_1) \\ \vdots & \ddots & \\ \Delta v_1(t_m) & \dots & \Delta v_{n-1}(t_m) \end{bmatrix} \in \mathbb{R}^{m \times (n-1)} \tag{55}$$

The matrix $\boldsymbol{V}$ can be factorised using principal component decomposition:

$$\boldsymbol{S} = \boldsymbol{V}\boldsymbol{W} \tag{56}$$

where $\boldsymbol{W} \in \mathbb{R}^{(n-1)\times(n-1)}$ is a matrix of column-wise eigenvectors of the matrix $\boldsymbol{V}^T\boldsymbol{V}$. The eigenvectors represent a new basis which factorises the matrix $\boldsymbol{V}$ into $n-1$ independent factors. The matrix $\boldsymbol{S} \in \mathbb{R}^{m\times(n-1)}$ denotes the empirical states of the independent factors.

In order to estimate a reduced factor model, we truncate the matrices such that $\boldsymbol{W}^* = \boldsymbol{W}[\{1, ..., n-1\}, \{1, ..., \beta\}] \in \mathbb{R}^{(n-1)\times\beta}$ and $\boldsymbol{S}^* = \boldsymbol{S}[\{1, ..., m\}, \{1, ..., \beta\}] \in \mathbb{R}^{m\times\beta}$. The matrix $\boldsymbol{V}^* = \boldsymbol{S}^*(\boldsymbol{W}^*)^T$ represents changes in FOMC policy rate change expectations corresponding to the reduced factor truncation. Let $s_j(t_a)$ be the (a, j) element of matrix $\boldsymbol{S}^*$ and let $w_{i,j}$ be the (i, j) element of matrix $\boldsymbol{W}$. Then:

$$\Delta v_i^*(t_a) = \sum_{j=1}^{\beta} s_j(t_a) w_{i,j} \tag{57}$$

From this the truncated jump states can be obtained as follows:

$$v_i^*(t_a) = \Delta v_i^*(t_a) + \begin{cases} v_i^*(t_{a-1}) & , t_{a-1} \notin \{x_0, ..., x_n\} \\ v_{i+1}^*(t_{a-1}) & , t_{a-1} \in \{x_0, ..., x_n\} \end{cases} \tag{58}$$

where the initial state is obtained from the calibration, i.e. $v_i^*(t_0) = v_i(t_0)$, therefore:

$$v_i^*(t_a) = v_i(t_0) + \sum_{a^*=1}^{a} \Delta v_{i^*}^*(t_{a^*}) = v_i(t_0) + \sum_{a^*=1}^{a}\sum_{j=1}^{\beta} s_j(t_{a^*}) w_{i,j} \tag{59}$$

where $i^* = i + \mathcal{A}_{t_{a^*}, t_a}$ denotes the number of FOMC meetings between t_{a^*} and t_a. Therefore the truncated forward rates can be written as follows:

$$\begin{aligned} f^*(t_a, T) &= f_0(t_a, T) + \sum_{i=1}^{n} \left(v_i(t_0) + \sum_{a^*=1}^{a}\sum_{j=1}^{\beta} s_j(t_{a^*}) w_{i,j} \right) \mathbb{1}(i \le \mathcal{A}_{t_a,T}) \\ &= f_0(t_a, T) + \sum_{i=1}^{n} \left(v_i(t_0) + \sum_{a^*=1}^{a}\sum_{j=1}^{\beta} s_j(t_{a^*}) w_{i,j} \right) \mathbb{1}(i \le \mathcal{A}_{t_a,T}) \\ &= f_0(t_a, T) + \sum_{i=1}^{n} v_i(t_0) \mathbb{1}(i \le \mathcal{A}_{t_a,T}) + \sum_{i=1}^{n}\sum_{a^*=1}^{a}\sum_{j=1}^{\beta} s_j(t_{a^*}) w_{i,j} \mathbb{1}(i \le \mathcal{A}_{t_a,T}) \\ &= f_0(t_a, T) + \sum_{i=1}^{n} v_i(t_0) \mathbb{1}(i \le \mathcal{A}_{t_a,T}) + \sum_{j=1}^{\beta}\sum_{i=1}^{n} w_{i,j} \mathbb{1}(i \le \mathcal{A}_{t_a,T}) \sum_{a^*=1}^{a} s_j(t_{a^*}) \end{aligned} \tag{60}$$

Taking the increment over time, for $t_{a-1} \notin \{x_0, ..., x_n\}$:

$$\begin{aligned}
\Delta f^*(t_a, T) &= f^*(t_a, T) - f^*(t_{a-1}, T) \\
&= f_0(t_a, T) + \sum_{i=1}^{n} v_i(t_0)\mathbb{1}(i \leq \mathcal{A}_{t_a,T}) + \sum_{j=1}^{\beta}\sum_{i=1}^{n} w_{i,j}\mathbb{1}(i \leq \mathcal{A}_{t_a,T}) \sum_{a^*=1}^{a} s_j(t_{a^*}) \\
&- f_0(t_{a-1}, T) - \sum_{i=1}^{n} v_i(t_0)\mathbb{1}(i \leq \mathcal{A}_{t_{a-1},T}) - \sum_{j=1}^{\beta}\sum_{i=1}^{n} w_{i,j}\mathbb{1}(i \leq \mathcal{A}_{t_{a-1},T}) \sum_{a^*=1}^{a-1} s_j(t_{a^*}) \\
&= \sum_{j=1}^{\beta}\sum_{i=1}^{n} w_{i,j}\mathbb{1}(i \leq \mathcal{A}_{t_a,T})\Big(\sum_{a^*=1}^{a} s_j(t_{a^*}) - \sum_{a^*=1}^{a-1} s_j(t_{a^*})\Big) \\
&= \sum_{j=1}^{\beta}\sum_{i=1}^{n} w_{i,j}\mathbb{1}(i \leq \mathcal{A}_{t_a,T}) s_j(t_a)
\end{aligned} \tag{61}$$

The above equation connects the empirical results to the model as follows. First write the forward rates without the drift component for a reduced factor model:[27]

$$\begin{aligned}
f(t, T) &\approx f(0, T) + \sum_{j=1}^{\beta}\sum_{i=1}^{n} \sigma_j \lambda_{i,j}\mathbb{1}(i \leq \mathcal{A}_{0,T}) W_j(t \wedge x_{\bar{i}(T)}) \\
&= f(0, T) + \sum_{j=1}^{\beta}\sum_{i=1}^{n} \lambda_{i,j}\mathbb{1}(i \leq \mathcal{A}_{0,T}) \sigma_j W_j(t \wedge x_{\bar{i}(T)})
\end{aligned} \tag{62}$$

Taking the increment between t_{a-1} and t_a in the case where $\mathcal{A}_{t_{a-1},t_a} = 0$

$$\begin{aligned}
\Delta f(t_a, T) &= f(t_a, T) - f(t_{a-1}, T) \\
&= f(0, T) + \sum_{j=1}^{n}\sum_{i=1}^{n} \lambda_{i,j}\mathbb{1}(i \leq \mathcal{A}_{0,T}) \sigma_j W_j(t_a \wedge x_{\bar{i}(T)}) \\
&- f(0, T) - \sum_{j=1}^{n}\sum_{i=1}^{n} \lambda_{i,j}\mathbb{1}(i \leq \mathcal{A}_{0,T}) \sigma_j W_j(t_{a-1} \wedge x_{\bar{i}(T)}) \\
&= \sum_{j=1}^{n}\sum_{i=1}^{n} \lambda_{i,j}\mathbb{1}(i \leq \mathcal{A}_{0,T}) \sigma_j \Big(W_j(t_a \wedge x_{\bar{i}(T)}) - W_j^P(t_{a-1} \wedge x_{\bar{i}(T)})\Big)
\end{aligned} \tag{63}$$

Now:

$$W_j(t_a \wedge x_{\bar{i}(T)}) - W_j(t_{a-1} \wedge x_{\bar{i}(T)}) = \begin{cases} W_j(t_a) - W_j(t_{a-1}) & , t_{a-1} < x_{\bar{i}(T)} \\ 0 & , t_a > x_{\bar{i}(T)} \end{cases} \tag{64}$$

Therefore:

$$W_j(t_a \wedge x_{\bar{i}(T)}) - W_j(t_{a-1} \wedge x_{\bar{i}(T)}) = \mathbb{1}(i \leq \mathcal{A}_{t_a,T})\big(W_j(t_a) - W_j(t_{a-1})\big) \tag{65}$$

[27] Ignoring the drift component is another approximating assumption of immaterial impact. Appendix C reports the size of the drift under the fitted model parameters — this is clearly negligible, especially since what matters for the present analysis is the increments in $f(t, T)$, i.e., $\Delta f(t_a, T)$ as considered below.

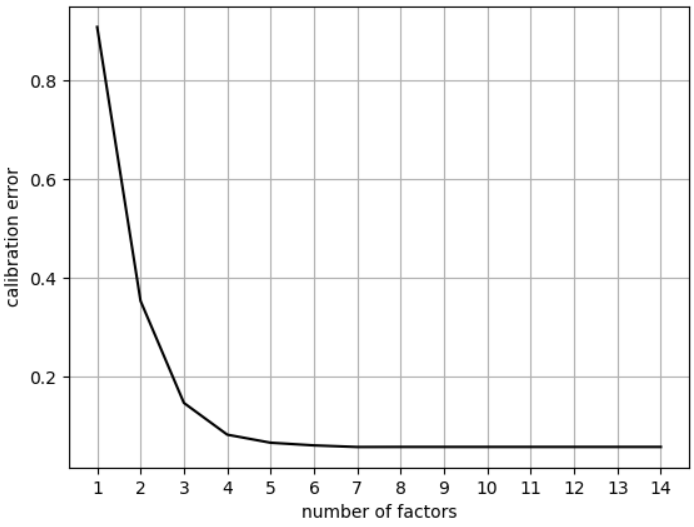

Figure 8: Total RMSE for each given number of factors

Let $\Delta W_j(t_a) = W_j(t_a) - W_j(t_{a-1})$, we can write:

$$\Delta f(t_a, T) = \sum_{j=1}^{n} \sum_{i=1}^{n} \lambda_{i,j} \mathbb{1}(i \leq \mathcal{A}_{t_a,T}) \sigma_j \Delta W_j(t_a) \tag{66}$$

Comparing equations Eq.(61) and Eq.(66) we find the empirical results are connected to the model with $w_{i,j} = \lambda_{i,j}$ and $s_j(t_a) = \sigma_j \Delta W_j(t_a)$.

4.1.2 Factor decomposition

Fitting the model to futures data as described above produces an empirical decomposition into the piecewise forward rate structures corresponding to the modelling approach proposed in this paper. The decomposition informs a dimension reduction achieved by removing factors which do not significantly impact the estimated dynamics. In order to choose the appropriate number of factors, consider the total root mean square error (RMSE) across all market instruments, i.e., define the total RMSE as:

$$e(\beta) = \sqrt{\sum_{a=1}^{m} \frac{O(t_a)}{m}} \tag{67}$$

where β is the number of factors used to obtain the forward rates from the calibration. Figure 8 suggests that over the sample period factors 8 and above do not improve the model fit. The model construction allows for inclusion of any number of factors, therefore below eight factors the number of factors becomes a choice between modelling accuracy and parsimony.

The estimated λ vectors reflect the empirical dynamics of policy rate expectations. Therefore they offer an interesting economic interpretation of the driving dynamics of forward rates, especially those with short maturities. Figure 9 shows the λ vectors corresponding to the top three factors. The factors reflect the general level across the term structure (factor 1), the gradient (factor 2) and curvature (factor 3). The

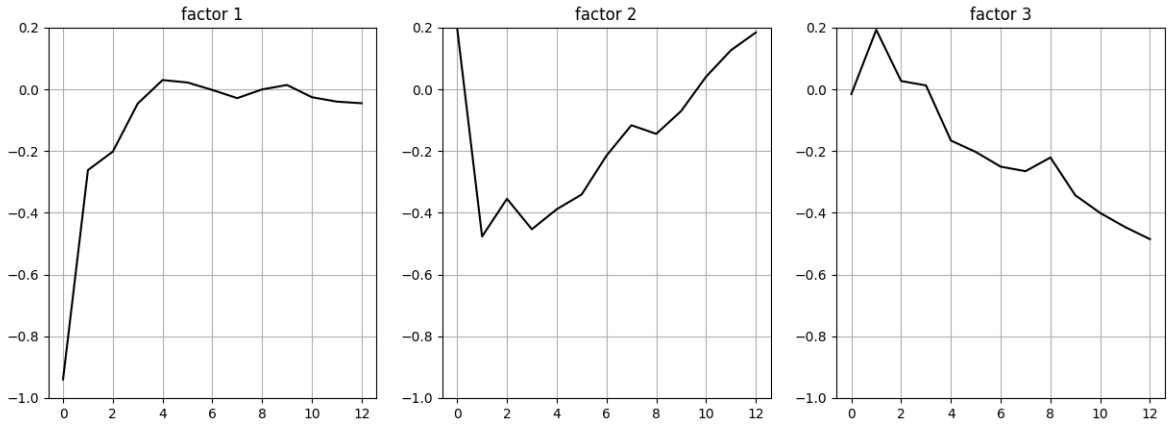

Figure 9: λ vectors for the first three factors

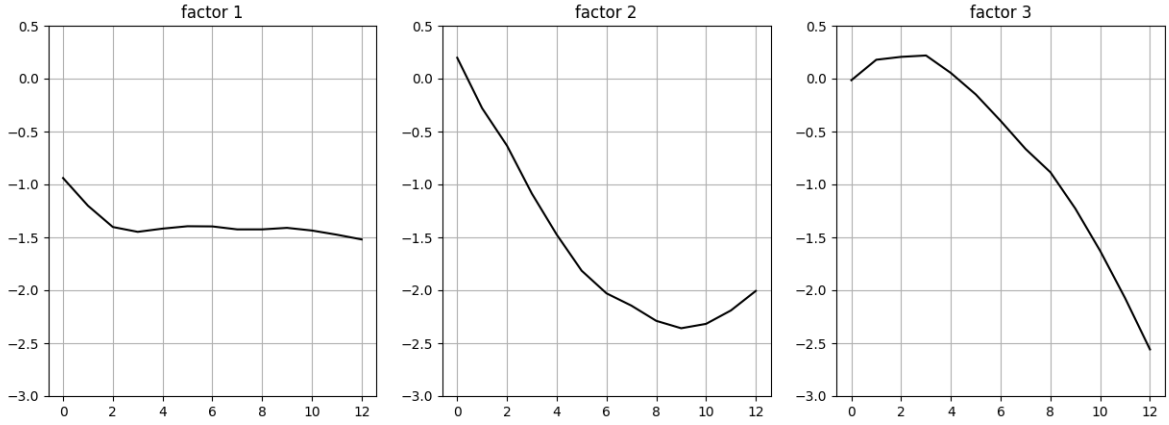

Figure 10: Forward rate level vectors for the first three factors

general shape of these vectors aligns with their parameterised counterparts in the Nelson/Siegel model (see Nelson and Siegel (1987)).

The modelling setup proposed in this paper interprets forward rates as an accumulation of expected policy rate changes. Therefore we can cast the decomposition weight vectors as factorised policy rate change expectations, where the resulting λ vectors correspond directly to factors in the proposed model. An interesting insight emerges regarding the dynamics of forward rates. As shown in Figure 9, the λ vector corresponding to factor 1 is concentrated mostly on the first element, revealing that parallel changes in the forward rate term structure are equivalent to changing expectations regarding the next FOMC policy rate change.

Although these results are based on the short end of the term structure, this connection can be conceptually extended to longer terms. Parallel changes have being long known to be the primary driver of term structure dynamics, these results reveal that parallel forward curve changes are directly related to changing expectations related to the first FOMC date. The connection between FOMC policy rate expectations and parallel changes in the forward curve is a key insight stemming from this modelling approach.

instrument	M0	M1	M2	M3	M4	M5	M6	Q0	Q1	Q2	Q3	Q4
1 factor	1.2	1.7	6.6	12.8	19.6	26.0	30.7	7.2	22.9	36.3	47.4	68.6
2 factor	1.1	1.4	1.5	1.4	2.2	2.6	2.6	0.8	2.1	1.9	5.0	10.6
3 factor	1.1	1.4	1.5	1.3	1.6	1.5	1.3	0.8	1.0	1.0	1.1	2.1
Skov & Skovmand	2.9	3.1	3.3	2.6	2.1	1.6	1.6	0.9	1.3	1.8	0.9	1.8

Table 1: RMSE table for monthly(M) and quarterly(Q) contracts. RMSE is expressed in basis points

The second factor is similarly concentrated on the first element, but with a distinctive change in the opposite direction for the remaining values. The magnitude of the first element is smaller than the sum of the remaining values, which gives rise to an opposite change in the forward rates between the first and last forward, with a smooth transition in between. For the forward curve this is a gradient change, which is typical for the second factor in term structure dynamics in the literature. The interpretation is that this captures dynamics where the expected aggregate changes (across all upcoming FOMC meeting dates) in policy rates do not change, but the expected timing of those changes does. For example, the expectations of a rate rise might increase for the next meeting, but the aggregate expected level does not change, so the expectations of rate rises decrease for subsequent meetings. An equivalent interpretation is that the second factor represents a negative correlation between the expectations related to the next policy rate change with the remaining term structure. Again this is a key insight, connecting FOMC policy rate change expectations with the behaviour of the second PCA factor for term structure changes.

The third factor, which appears as a curvature change in the forward rate term structure, is actually quite similar to the second factor. It also represents a negative correlation involving the next policy rate change. However, for the third factor this is focused mostly on the relationship to the second FOMC meeting, rather than the entire remaining term structure. Specifically, this relates to the expected aggregate outcome over the next *two* FOMC meetings remaining fairly constant, while allowing for uncertainty regarding the timing of the change.

4.1.3 Model fit to futures prices

A notable feature of the RMSE shown in Figure 8 is that it does not converge to zero, meaning that even a full factor model is not able to perfectly calibrate to futures prices. This is because we are only focusing on the primary aspect, i.e., modelling jumps at FOMC meeting dates.[28] From this perspective, consider the RMSE for each futures:

$$e_j^x(\beta) = \sqrt{\frac{\sum_a (\hat{F}_j^x(t_a) - F_j^x(t_a))^2}{m}} \tag{68}$$

Table 1 gives the RMSE for the seven one–month and five quarterly futures used by Skov and Skovmand (2021) in the estimation of a traditional diffusive, three–factor Gaussian model, based on the same data period as that paper. The Skov and Skovmand (2021) results are reproduced in the final row, while the first three rows present the RMSEs for the one–, two– and three–factor versions of our Gaussian model, respectively. Thus the most appropriate comparison to Skov and Skovmand (2021) is the three–factor version of our model, demonstrating the impact of moving to a model with scheduled jumps on FOMC meeting dates: There is a clear improvement in the RMSE for one–month futures at the near end of

[28] Modelling a diffusive residual spread and/or the possibility of SOFR (extensions which were considered in Gellert and Schlögl (2021), for example) would introduce additional freedom to allow for a perfect fit.

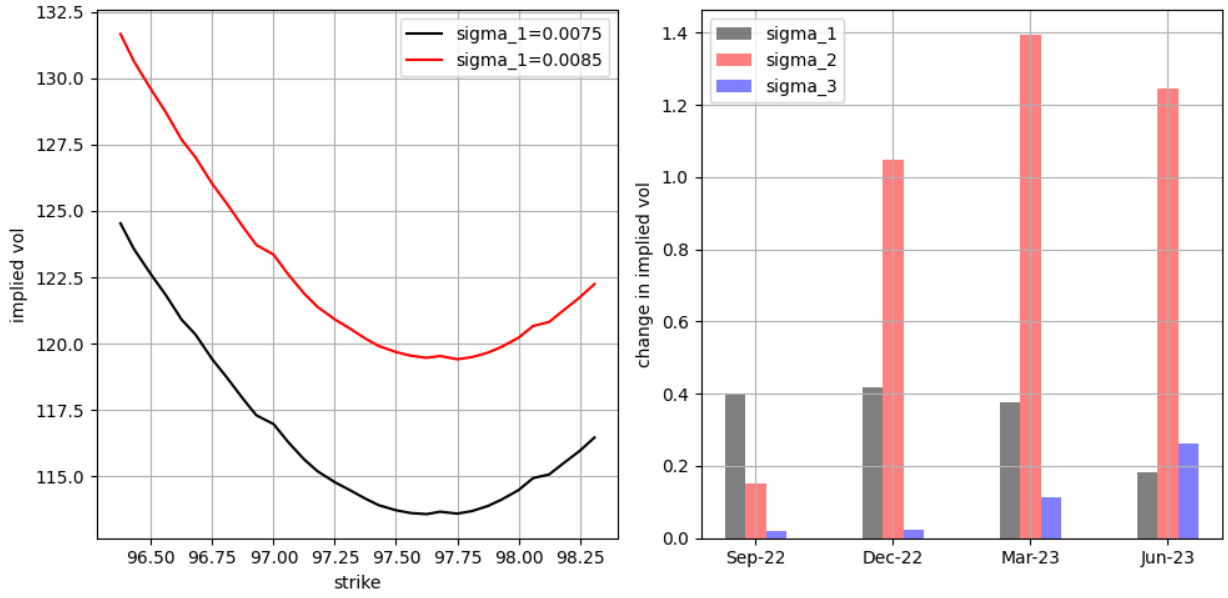

Figure 11: (LHS) Implied volatility for different values of σ. (RHS) ATM implied volatility sensitivity across contracts to changes in σ.

the term structure, while this improvement is absent for quarterly futures and the far end of the term structure.[29]

4.2 Calibrating the stochastic volatility model

4.2.1 Factor Sensitivities

The first four moments of terminal distributions (for all relevant maturities) to a large part determine the quality of fit in cross–sectional calibration of a term structure model to interest rate options. A terminal (risk–neutral) distribution at a specific expiry can be characterised in terms of implied volatilities across different strikes. In this representation, the first moment corresponds to a horizontal shift in the implied volatilities (across strikes), the second moment to a vertical shift (across all implied volatilities), the third moment to a change in the slope of the implied volatility curve, and the fourth moment to a change in the convexity. Using this characterisation, one can illustrate the flexibility of the model proposed in this paper to control the moments of the distribution as well as their term structures across different expiries.

Using a model calibration on the 10-June-2022 to the first four quarterly SOFR futures options, including all available strikes, we study the sensitivity of implied volatilities to the model parameters. Starting with σ, see Figure 11, it is apparent that changing this variable results in a parallel shift in the implied volatilities, thereby controlling the second moment. The right–hand graph in Figure 11 shows how different factors impact different expiries, with factor 1 focused on short–term expiries, while factors 2 and 3 increasingly focus on the longer expiries, providing calibration flexibility across the term structure.

The α parameter determines the level of stochastic volatility in the models, usually associated with the fourth moment. As shown in Figure 12, changing the α parameter results in a change in convexity as well

[29] It is worth noting that using a different modelling approach (directly modelling scheduled jumps as normally distributed with a stochastically evolving mean) and conducting a full econometric estimation based on maximum likelihood in conjunction with the Kalman filter, Schlögl, Skov and Skovmand (2023) arrive at a similar conclusion.

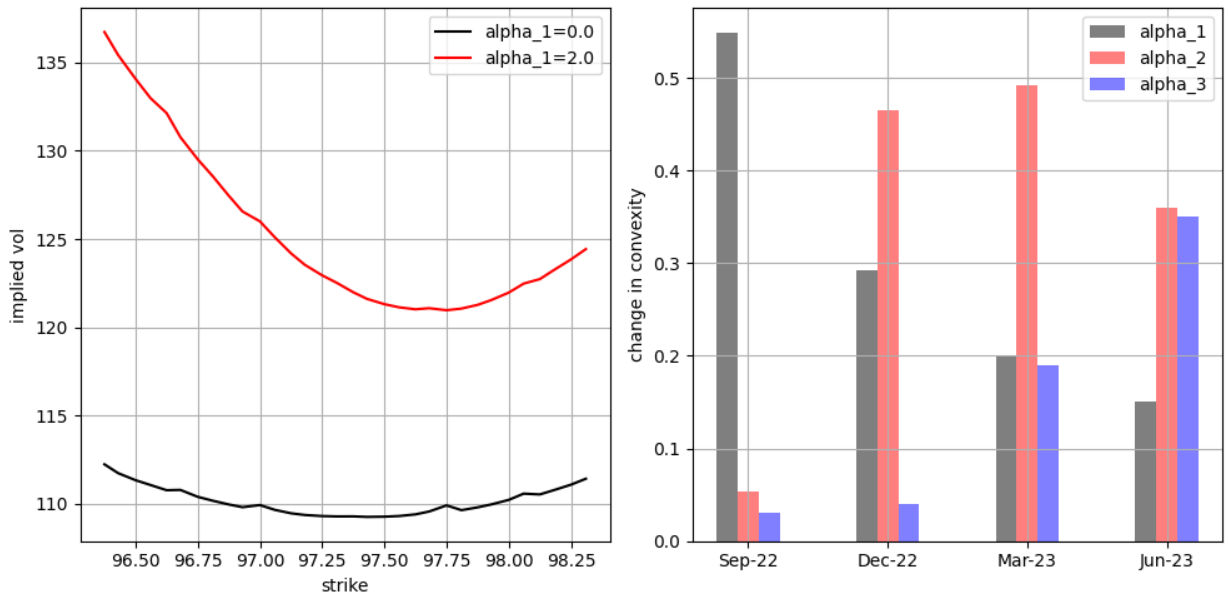

Figure 12: (LHS) Implied volatility for different values of α. (RHS) Implied volatility convexity sensitivity across contracts to changes in α.

as the level of volatilities. Control of just convexity, without changing at–the–money (ATM) volatilities, is possible by combining offsetting changes in the σ parameter. The right–hand graph in Figure 12 shows different impacts on convexity from different factors across expiries, enabling the model to calibrate to stochastic volatility term structures.

The ρ parameter determines the correlation between stochastic volatility and the forward rates. As can be seen in Figure 13, changing the ρ parameter results in a gradient change in implied volatilities, corresponding to a change in the third moment. Similarly to the other parameters, the impact on implied volatility skewness varies for different factors across expiries, allowing the model be calibrated to different correlation term structures.

λ and θ are two variables associated with mean reversion. The λ parameter controls mean reversion of the forward rates while the θ parameter controls the mean reversion of the stochastic volatility. From an implied volatility perspective, as shown in Figure 14, the mean reversion parameters work in reverse to their corresponding volatility parameters. The λ parameters offset the impact from σ and result in a parallel change in implied volatility with the opposite sign to the change in the parameter. The θ parameter reverses the α parameter and therefore results in both a level and convexity change in the implied volatilities.

Thus, the model proposed has the flexibility to attempt simultaneous calibration to option–implied volatilities across both strikes and expiries. Additional flexibility for calibration comes from the ability to define the parameters as functions of time.

4.2.2 Cross–sectional fit to options on SOFR futures

In practical applications, in particular derivative pricing and risk management, the ability to calibrate to cross–sectional (i.e., market prices at a single point in time, as opposed to time series) option data is an important feature of interest rate models. Although it violates the model assumptions, it is standard practice in industry to recalibrate interest rate models on a daily basis to liquidly traded instruments.

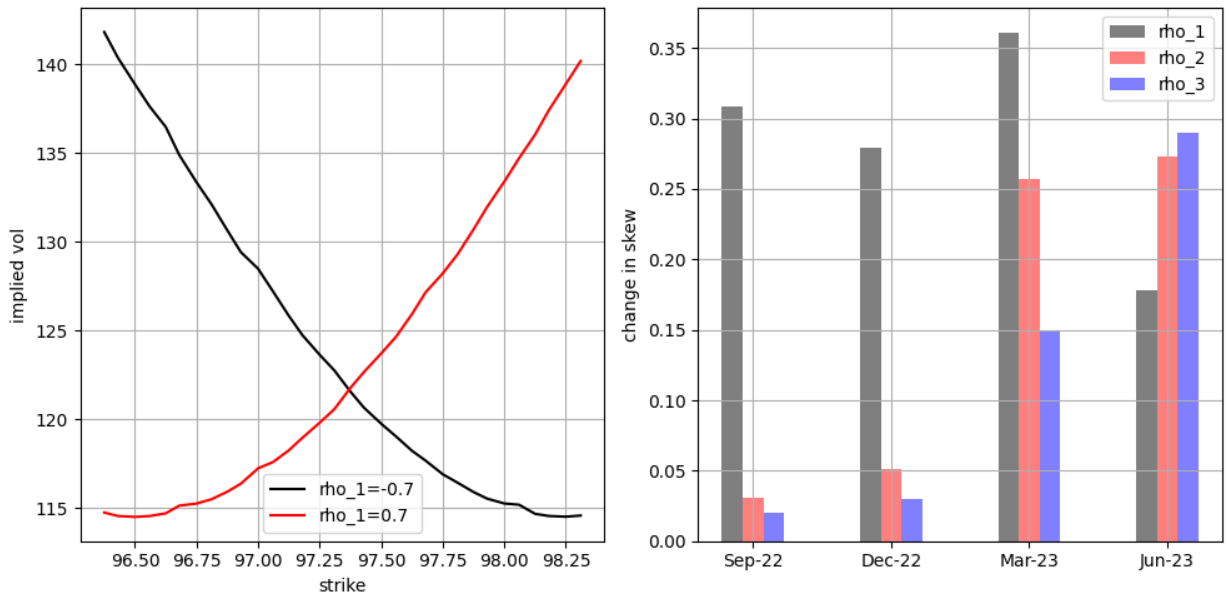

Figure 13: (LHS) Implied volatility for different values of ρ. (RHS) Implied volatility skew sensitivity across contracts to changes in ρ.

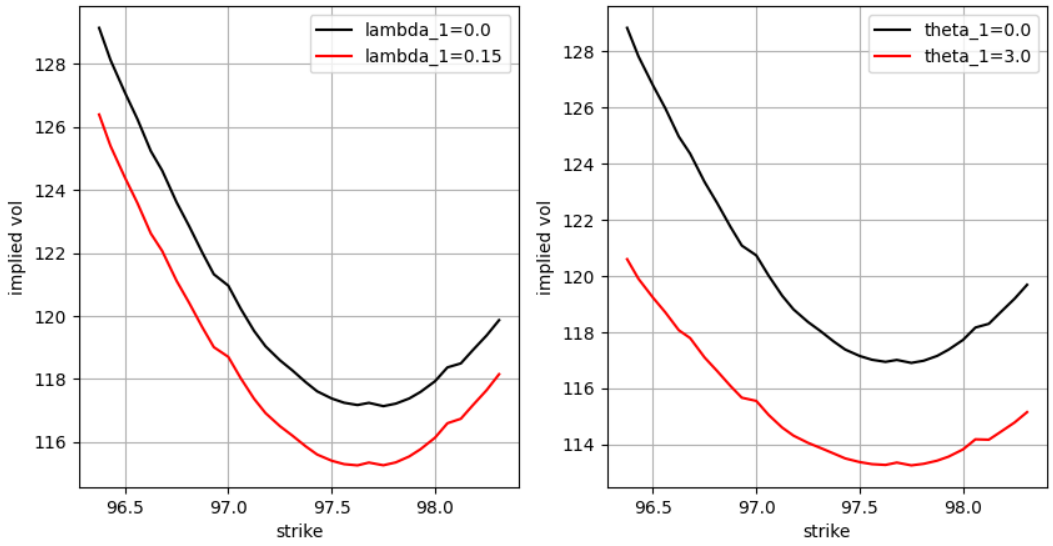

Figure 14: Varying lambda and theta.

Options on SOFR futures have been one of the first SOFR–related option instruments to trade since the inception of the new benchmark. These are also the only SOFR–related options traded directly on an exchange, meaning that the price information is widely available.

At the time of writing, most of the market liquidity in options on SOFR futures is concentrated on the front four options on three–month SOFR futures. Arguably, shorter expiry interest rate options are the most difficult to fit, due to steep and highly variable term structures in implied volatilities and implied

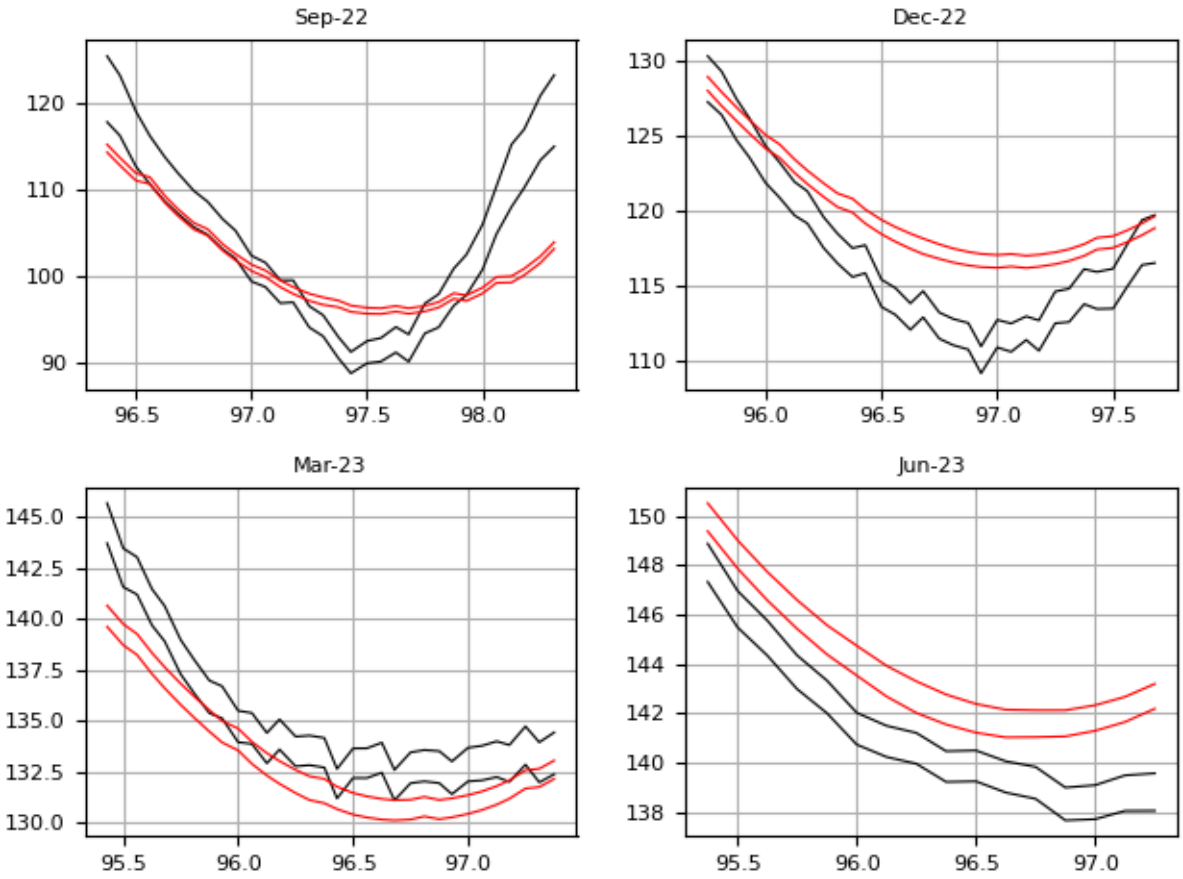

Figure 15: Calibration with constant parameters. Graphs show Bachelier implied volatilities, where market implied volatilities are in black and model implied volatilities are in red.

kurtosis, as is evident in the data set used for this section. This makes calibration to these options a good proof of concept in this respect.

For the calibration, we take the γ parameters from the estimation performed in Section 4.1. The remaining parameters σ, α, λ, θ and ρ are calibrated to option prices. In the calibration, σ controls the general level of volatility, and the mean reversion parameter λ gives some control of volatility levels across expiries. α controls the level of kurtosis, and the stochastic volatility mean reversion parameter α gives some control of kurtosis across expiries. The correlation parameter ρ controls the implied volatility skew.

Each of the model calibration parameters can be defined as a function of time. Combined with the ability to choose the number of HJM factors, this provides significant flexibility in the model for calibration. We begin by performing the calibration with the parameters constant across time before adding time dependent parameters. The results are presented as a comparison of normal (i.e., "Bachelier") volatilities implied from the bid/offer prices taken from settlement price information on the 10-June-2022, with the 5% confidence interval for the calibrated model price based on simulation results.

The calibration results shown in Figure 15 show that the model can be fitted to general volatility levels, skew and convexity, though insufficiently to match market–implied volatilities exactly. An important feature of market–implied volatilities is the sharply declining convexity as a function of expiry. Another feature is the term structure in skew slightly declining as a function of expiry. As can be seen in Table

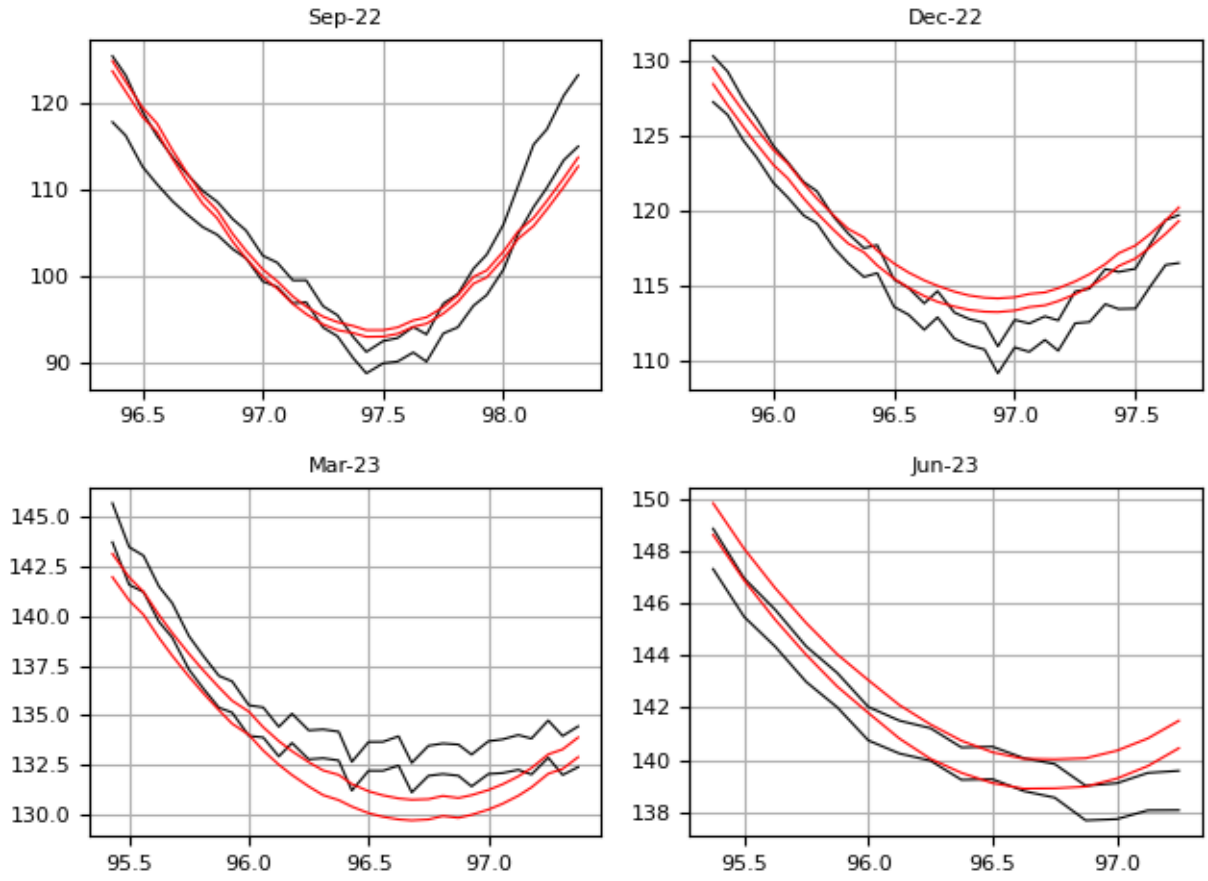

Figure 16: Calibration with time dependent parameters. Graphs show Bachelier implied volatilities, where market implied volatilities are in black and model implied volatilities are in red.

2, with constant parameters the calibration focuses on α_0, which is the stochastic volatility parameter associated with the first factor. This understates the convexity on the first expiry and overstates for the longest expiry, thus effectively freezing factor 2 and 3 stochastic volatility (α_1, α_2) at zero. These results suggest the introduction of time dependent stochastic volatility parameters.

We define stochastic volatility parameters as a function of t, piecewise constant between the option expiry dates. As shown in Figure 16, this change provides enough flexibility across different expiries to result in a substantial improvement in model fit. With the added time dependence, the first stochastic volatility parameter α_0 has increased for short expiries and decreased for longer expiries, as opposed to the results obtained with constant parameters.

This example demonstrates the flexibility of the model. Based on the calibration with constant parameters, we were able to make an informed choice with respect to which parameters could be made time dependent to benefit the calibration. We only had to change three of the fifteen available parameters to achieve a much better calibration results, albeit for a limited set of calibration instruments. This same approach could be repeated for a larger set of calibration instruments, making other parameters time dependent or increasing the number the factors if required.

parameters	σ_1	σ_2	σ_3	λ_1	λ_2	λ_3	α_1	α_2	α_3	ρ_1	ρ_2	ρ_3	θ_1	θ_2	θ_3
constant	0.0081	0.006	0.0041	0.01	0	0.16	1.57	0.82	0	-0.2	0	0	0	0	0
time dependent	0.00663	0.00587	0.00447	0.02	0.004	0.35	[3.142, 1.35, 3.2, 0.86]	[0.76, 0.66, 0.6, 0.22]	[3.0, 0.6, 0.5, 4.1]	-0.14	-0.025	-0.83	0.1	0	11.0

Table 2: Calibrated model parameters.

5 Further implications of the model

5.1 Implied volatility behaviour during the accrual period

A prevalent approach in the LIBOR to SOFR transition, as reflected in literature (see Lyashenko and Mercurio (2019)), is the adaptation of existing LIBOR–based modelling to SOFR. A highly practical problem stemming from this approach is the behaviour of options in the accrual period of the SOFR term rate, i.e. for term forwards $S(T_i, T_k)$ at time $T_i < t \leq T_k$. This occurs when the expiry of the option is set past the beginning of the accrual period.

Examples of impacted options are in–arrears SOFR caps and exchange–traded options on 1M SOFR futures.[30] Existing LIBOR–based pricing models require an artificially induced decay of the "SOFR term rate" volatility within its accrual period, because as this rate accrues, its value because more and more known. To achieve this effect, Lyashenko and Mercurio (2019) suggest having volatility linearly decay during the accrual period.

In contrast, the model proposed in this paper handles the case of partially set compounded or averaged SOFR naturally, and also provides an alternative insight into the decay characteristics of implied volatility within the accrual period. As shown in Figure 17, setting a constant volatility level σ and removing the indicator functions in the HJM volatility function results in a linearly decaying implied volatility. This is consistent with the *ad hoc* assumption in Lyashenko and Mercurio (2019), but here it results directly from model behaviour.

However, a different behaviour of implied volatility appears when forward rate volatility is driven by FOMC meetings and therefore there is zero volatility between the last FOMC meeting within the accrual period and the end of the accrual period. As shown in Figure 17, this results in an accelerating decay in implied volatility, hitting zero at the final meeting date prior to the end of the accrual period. Note that this analysis does ignore volatility of the SOFR to policy target rate spread, but this is a second–order effect. Spread volatility contributes relatively little to the variance of SOFR, suggesting the qualitative implication on the accrual period behaviour of option–implied volatility is likely to be accurate — a prediction of the model which can be verified once options on 1M SOFR futures become sufficiently liquid in the market.

5.2 Mean reversion vs. policy rate expectations

Mean reversion is embedded in the model in the definition of forward rate volatilities $\sigma_j(t,T)$, which can be rewritten as follows:

$$\sigma_j(t,T) = \sigma_j(t)\sqrt{v_j(t)}\exp\Big(-\int_t^T \lambda_j(s)ds\Big)\sum_{i=1}^{n}\mathbb{I}_{\{i\leq\mathcal{A}(t,T)\}}\gamma_{i,j} \tag{69}$$

On the one hand, mean reversion is reflected in the term $\exp\Big(-\int_t^T \lambda_j(s)ds\Big)$, resulting in the volatility of instantaneous forward rates decaying as a function of time to maturity $(T-t)$. On the other hand, the

[30] Options on 3M futures expire prior to the accrual period, hence are not impacted by behaviour during the accrual period.

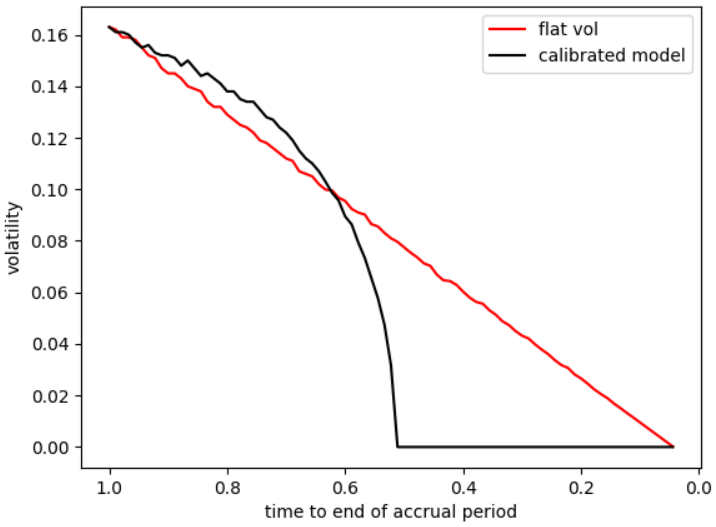

Figure 17: Accrual period term volatility comparison

$\gamma_{i,j}$ vector scales the volatility function based on the number of FOMC meetings between t and T and as such has an inherent dependence on $T-t$. Therefore, for a given $\lambda_j(s)$ function, it is possible to define $\gamma_{i,j}$ such that:

$$\sum_{i=1}^{n} \mathbb{I}_{\{i \leq \mathcal{A}(t,T)\}} \gamma_{i,j} \approx \exp\left(- \int_t^T \lambda_j(s) ds \right) \tag{70}$$

That is, it is possible to set $\lambda_j = 0$ and mimic mean reverting dynamics with the appropriate choice of $\gamma_{i,j}$. In Section 4.1, the $\gamma_{i,j}$ were derived by PCA of forward rate states implied from SOFR futures. The first factor, i.e for $j = 1$, explains a large proportion (around 80%) of the forward state variance. It has a clear economic interpretation of focusing forward rate dynamics on the changing expectations related to the change in policy rate at the FOMC date immediately following t. This in itself is an intuitively agreeable insight: forward rate dynamics are largely driven by changing expectations of the next move in the policy rate. Furthermore, when $\gamma_{i,j}$ has the opposite sign between $\gamma_{1,1}$ and $\gamma_{i,1}$ for $i > 1$, this mimics mean reverting behaviour in the sense that the market expects a policy rate hike to be followed by a drop and vice versa. Inspection of the empirically derived $\gamma_{i,j}$ vector for $j = 1$ reveals that it is now possible to choose $\lambda_j(s)$ such that:

$$\exp\left(- \int_t^T \lambda_j(s) ds \right) \approx \sum_{i=1}^{n} \mathbb{I}_{\{i \leq \mathcal{A}(t,T)\}} \gamma_{i,j} \tag{71}$$

by setting:

$$\lambda_j(s) = \begin{cases} 0.9, & s - t < 0.5 \\ 0.08, & \text{otherwise} \end{cases} \tag{72}$$

which results in the comparison shown in Figure 18, demonstrating it how it is possible to obtain the behaviour implied by the (PCA–derived) γ from an appropriate choice of $\lambda_j(s)$. It is clear that most of

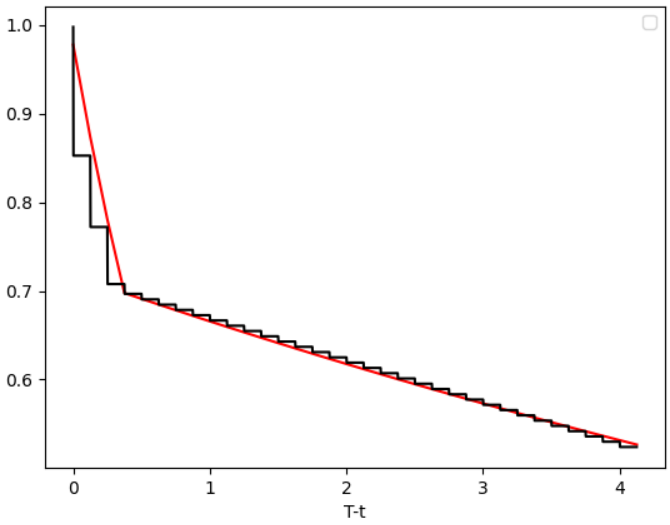

Figure 18: Comparison of $\exp\left(-\int_t^T \lambda_j(s)ds\right)$(red) and $\sum_{i=1}^n \mathbb{I}_{\{i\leq\mathcal{A}(t,T)\}}\gamma_{i,j}$(black)

the difference stems from the continuous and piecewise definitions, but both approaches are very similar in terms of embedding mean reversion dynamics. Thus, the model reflects an implicit connection between forward rate dynamics driven by expectations of policy rate changes and mean reverting behaviour of the short rate.

6 Conclusion

Having observed that empirically the short rate (EFFR or SOFR) follows dynamics determined primarily by jumps at known times, but forward rates follow primarily diffusive dynamics, we have constructed a model which reconciles these two (naively contradictory) observations. Such a model is needed because, with the transition away from the LIBOR benchmark, fixed income instruments referencing SOFR are becoming increasingly important. In addition, the actions of the Federal Reserve in response to the 2008 financial crisis over the last decade have removed much of the daily volatility from the EFFR, long thought of as the best empirical proxy for the short rate. This reduction in volatility has revealed an underlying structure of short rates consisting of discontinuities directly related to FOMC policy target rate changes, which is also reflected in the empirical dynamics of SOFR. For the steps in the target rate modelled in this fashion, a possible economic interpretation is that there is a fundamental "shadow" rate of interest evolving diffusively. Only the central bank observes this shadow rate (perhaps imperfectly), and at known dates updates the central bank target rate to match this shadow rate.

Fitting a model based on scheduled jumps to a history of SOFR futures prices has revealed a connection between interest rate mean reversion and FOMC policy rate expectations: It turns out that the volatility component modelling jump behaviour at FOMC meeting dates mimics instantaneous forward rate volatility decaying in time to maturity and therefore has a similar effect as traditional mean reversion in the model. This reveals a direct connection between the evolution of FOMC policy rate expectations reflected in SOFR futures prices and traditional modelling of mean reverting interest rate dynamics: The primary driver of SOFR futures prices are changes in expectations related to the next FOMC meeting,

which in turn tends to be negatively correlated with changes in expectations for subsequent meetings, creating variance decay as a function of time to maturity. Historically, the Federal Reserve in managing economic cycles acts to mean revert interest rates. The market expects the Federal Reserve to continue to act this way, and using our modelling set–up this expectation is actually detectable in the evolution of SOFR futures prices.

In the context of cross–sectional calibration, stochastic volatility allows the model to fit skewness and convexity across strikes, a prominent feature in interest rate option prices. We demonstrated this on options on SOFR futures. The model also could be adapted to other calibration instruments, such as caps and swaptions.

Appendix A Bond price derivation

A.1 Single dimensional case

Define the following:

$$\sigma(t,T) = \chi(t)\phi(T) \tag{73}$$

$$\phi(T) = \exp\Big(- \int_0^T \lambda(v)dv \Big) \tag{74}$$

$$\chi(t) = \sigma(t)\exp\Big(\int_0^t \lambda(v)dv \Big) \tag{75}$$

$$\Lambda(t,T) = \int_t^T \exp\Big(- \int_t^u \lambda(v)dv \Big) du \tag{76}$$

$$\Phi(t) = \int_0^t \sigma^2(s)\exp\Big(- 2\int_s^t \lambda(v)dv \Big) ds \tag{77}$$

HJM result:

$$
\begin{aligned}
f(t,T) &= f(0,T) + \int_0^t \sigma(s,T) \int_s^T \sigma(s,u) du ds + \int_0^t \sigma(s,T) dW(s) \\
&= f(0,T) + \int_0^t \chi(s)\phi(T) \int_s^T \chi(s)\phi(u) du ds + \int_0^t \chi(s)\phi(T) dW(s) \\
&= f(0,T) + \int_0^t \sigma(s) \exp\Big(\int_0^s \lambda(v) dv \Big) \exp\Big(- \int_0^T \lambda(v) dv \Big) \\
&\times \int_s^T \sigma(s) \exp\Big(\int_0^s \lambda(v) dv \Big) \exp\Big(- \int_0^u \lambda(v) dv \Big) du ds \\
&+ \int_0^t \sigma(s) \exp\Big(\int_0^s \lambda(v) dv \Big) \exp\Big(- \int_0^T \lambda(v) dv \Big) dW(s) \\
&= f(0,T) + \int_0^t \sigma^2(s) \exp\Big(- \int_s^T \lambda(v) dv \Big) \int_s^T \exp\Big(- \int_s^u \lambda(v) dv \Big) du ds \\
&+ \int_0^t \sigma(s) \exp\Big(- \int_s^T \lambda(v) dv \Big) dW(s) \\
&= f(0,T) + \int_0^t \sigma^2(s) \exp\Big(- \int_s^T \lambda(v) dv \Big) \Lambda(s,T) ds + \int_0^t \sigma(s) \exp\Big(- \int_s^T \lambda(v) dv \Big) dW(s)
\end{aligned}
$$

let $y(t) = \int_0^t \sigma^2(s)\exp\Big(-\int_s^t \lambda(v)dv\Big)\Lambda(s,t)ds + \exp\Big(\int_t^T \lambda(v)dv\Big)\int_0^t \sigma(s)\exp\Big(-\int_s^T \lambda(v)dv\Big)dW(s)$ substitute $\int_0^t \sigma(s)\exp\Big(-\int_s^T \lambda(v)dv\Big)dW(s) = \frac{y(t)-\int_0^t \sigma^2(s)\exp\Big(-\int_s^t \lambda(v)dv\Big)\Lambda(s,t)ds}{\exp\Big(\int_t^T \lambda(v)dv\Big)}$

$$
\begin{aligned}
f(t,T) &= f(0,T) + \int_0^t \sigma^2(s)\exp\Big(-\int_s^T \lambda(v)dv\Big)\Lambda(s,T)ds + \int_0^t \sigma(s)\exp\Big(-\int_s^T \lambda(v)dv\Big)dW(s) \\
&= f(0,T) + \exp\Big(-\int_t^T \lambda(v)dv\Big)y(t) + \int_0^t \sigma^2(s)\exp\Big(-\int_s^T \lambda(v)dv\Big)\Lambda(s,T)ds \\
&- \exp\Big(-\int_t^T \lambda(v)dv\Big)\int_0^t \sigma^2(s)\exp\Big(-\int_s^t \lambda(v)dv\Big)\Lambda(s,t)ds \\
&= f(0,T) + \exp\Big(-\int_t^T \lambda(v)dv\Big)y(t) + \exp\Big(-\int_t^T \lambda(v)dv\Big) \\
&\times \int_0^t \sigma^2(s)\Big\{\exp\Big(\int_t^T \lambda(v)dv\Big)\exp\Big(-\int_s^T \lambda(v)dv\Big)\Lambda(s,T) - \exp\Big(-\int_s^t \lambda(v)dv\Big)\Lambda(s,t)\Big\}ds \\
&= f(0,T) + \exp\Big(-\int_t^T \lambda(v)dv\Big)y(t) + \exp\Big(-\int_t^T \lambda(v)dv\Big) \\
&\times \int_0^t \sigma^2(s)\exp\Big(-\int_s^t \lambda(v)dv\Big)\Big\{\Lambda(s,T) - \Lambda(s,t)\Big\}ds \\
&= f(0,T) + \exp\Big(-\int_t^T \lambda(v)dv\Big)y(t) \\
&+ \Lambda(t,T)\exp\Big(-\int_t^T \lambda(v)dv\Big)\int_0^t \sigma^2(s)\exp\Big(-2\int_s^t \lambda(v)dv\Big)ds \\
&= f(0,T) + \exp\Big(-\int_t^T \lambda(v)dv\Big)y(t) + \Phi(t)\Lambda(t,T)\exp\Big(-\int_t^T \lambda(v)dv\Big)
\end{aligned}
$$

therefore:

$$
\begin{aligned}
\int_t^T f(t,u)du &= \int_t^T \Big(f(0,u) + \exp\Big(-\int_t^u \lambda(v)dv\Big)y(t) + \Phi_j(t)\Lambda(t,u)\exp\Big(-\int_t^u \lambda(v)dv\Big)\Big)du \\
&= \int_t^T f(0,u)du + y(t)\int_t^T \exp\Big(-\int_t^u \lambda(v)dv\Big)du + \Phi(t)\int_t^T \Lambda(t,u)\exp\Big(-\int_t^u \lambda(v)dv\Big)du \\
&= \int_t^T f(0,u)du + \Lambda(t,T)y(t) + \Phi(t)\int_t^T \Lambda(t,u)d\Lambda(t,u) \\
&= \int_t^T f(0,u)du + \Lambda(t,T)y(t) + \frac{1}{2}\Phi(t)\Lambda^2(t,T)
\end{aligned}
$$

Therefore, the bond price is given by

$$
B(t,T) = \exp\Big(-\int_t^T f(t,u)du\Big) = \frac{B(0,T)}{B(0,t)}\exp\Big(-\Lambda(t,T)y(t) - \frac{1}{2}\Phi(t)\Lambda^2(t,T)\Big) \tag{78}
$$

A.2 Single dimensional case with piecewise continuous short rate

Define the following:

$$\sigma(t,T) = \sum_{i=1}^{n} \mathbb{I}_{\{i \leq \mathcal{A}(t,T)\}} \chi(t)\phi(T)\gamma_i \tag{79}$$

$$\phi(T) = \exp\Big(- \int_0^T \lambda(v)dv \Big) \tag{80}$$

$$\chi(t) = \sigma(t)\exp\Big(\int_0^t \lambda(v)dv \Big) \tag{81}$$

$$\Lambda(t,T) = \int_t^T \exp\Big(- \int_t^u \lambda(v)dv \Big) du \tag{82}$$

$$\Lambda_a(t,T) = \int_a^T \exp\Big(- \int_t^u \lambda(v)dv \Big) du \tag{83}$$

$$\Phi(t) = \int_0^t \sigma^2(s)\exp\Big(- 2\int_s^t \lambda(v)dv \Big) ds \tag{84}$$

A.2.1 trivial case $t < T < x_1$

HJM result:

$$f(t,T) = f(0,T) + \int_0^t \sigma(s,T) \int_t^T \sigma(s,u)duds + \int_0^t \sigma(s,T)dW(s) = f(0,T) \tag{85}$$

$$\int_t^T f(t,u)du = \int_t^T f(0,u)du \tag{86}$$

Therefore, the bond price is given by

$$B(t,T) = \exp\Big(- \int_t^T f(t,u)du \Big) = \frac{B(0,T)}{B(0,t)} \tag{87}$$

A.2.2 basic case $t < x_1 < T < x_2$

$$\int_t^T f(t,u)du = \int_t^{x_1} f(t,u)du + \int_{x_1}^T f(t,u)du \tag{88}$$

$$= \int_t^{x_1} f(0,u)du + \int_{x_1}^T f(t,u)du \tag{89}$$

To solve $\int_{x_1}^{T} f(t,u)du$, restrict $T \in [x1, x2]$ and $t < x_1$, HJM result:

$$
\begin{aligned}
f(t,T) &= f(0,T) + \int_0^t \sigma(s,T) \int_s^T \sigma(s,u) du ds + \int_0^t \sigma(s,T) dW(s) \\
&= f(0,T) + \int_0^t \sum_{i=1}^{n} \mathbb{I}_{\{i \le \mathcal{A}(s,T)\}} \chi(s)\phi(T)\gamma_i \int_s^T \sum_{j=1}^{n} \mathbb{I}_{\{j \le \mathcal{A}(s,u)\}} \chi(s)\phi(u)\gamma_j du ds \\
&+ \int_0^t \sum_{i=1}^{n} \mathbb{I}_{\{i \le \mathcal{A}(s,T)\}} \chi(s)\phi(T)\gamma_i dW(s) \\
&= f(0,T) + \int_0^t \chi(s)\phi(T)\gamma_1 \int_s^T \mathbb{I}_{\{s<x_1\}} \mathbb{I}_{\{u>x_1\}} \chi(s)\phi(u)\gamma_1 du ds + \int_0^t \chi(s)\phi(T)\gamma_1 dW(s) \\
&= f(0,T) + \gamma_1^2 \int_0^t \chi(s)\phi(T) \mathbb{I}_{\{s<x_1\}} \int_s^T \mathbb{I}_{\{u>x_1\}} \chi(s)\phi(u) du ds + \gamma_1 \int_0^t \chi(s)\phi(T) dW(s) \\
&= f(0,T) + \gamma_1^2 \int_0^t \chi(s)\phi(T) \int_s^T \mathbb{I}_{\{u>x_1\}} \chi(s)\phi(u) du ds + \gamma_1 \int_0^t \chi(s)\phi(T) dW(s) \\
&= f(0,T) + \gamma_1^2 \int_0^t \chi(s)\phi(T) \int_{x_1}^T \chi(s)\phi(u) du ds + \gamma_1 \int_0^t \chi(s)\phi(T) dW(s) \\
&= f(0,T) + \gamma_1^2 \int_0^t \sigma(s) \exp\Big(\int_0^s \lambda(v) dv \Big) \exp\Big(- \int_0^T \lambda(v) dv \Big) \\
&\times \int_{x_1}^T \sigma(s) \exp\Big(\int_0^s \lambda(v) dv \Big) \exp\Big(- \int_0^u \lambda(v) dv \Big) du ds \\
&+ \gamma_1 \int_0^t \sigma(s) \exp\Big(\int_0^s \lambda(v) dv \Big) \exp\Big(- \int_0^T \lambda(v) dv \Big) dW(s) \\
&= f(0,T) + \gamma_1^2 \int_0^t \sigma^2(s) \exp\Big(- \int_s^T \lambda(v) dv \Big) \int_{x_1}^T \exp\Big(- \int_s^u \lambda(v) dv \Big) du ds \\
&+ \gamma_1 \int_0^t \sigma(s) \exp\Big(- \int_s^T \lambda(v) dv \Big) dW(s) \\
&= f(0,T) + \gamma_1^2 \int_0^t \sigma^2(s) \exp\Big(- \int_s^T \lambda(v) dv \Big) \Lambda_{x_1}(s,T) ds + \gamma_1 \int_0^t \sigma(s) \exp\Big(- \int_s^T \lambda(v) dv \Big) dW(s)
\end{aligned}
$$

let

$$
y(t) = \gamma_1^2 \int_0^t \sigma^2(s) \exp\Big(- \int_s^t \lambda(v) dv \Big) \Lambda_{x_1}(s,t) ds + \exp\Big(\int_t^T \lambda(v) dv \Big) \gamma_1 \int_0^t \sigma(s) \exp\Big(- \int_s^T \lambda(v) dv \Big) dW(s) \tag{90}
$$

substitute

$$
\gamma_1 \int_0^t \sigma(s) \exp\Big(- \int_s^T \lambda(v) dv \Big) dW(s) = \frac{y(t) - \gamma_1^2 \int_0^t \sigma^2(s) \exp\Big(- \int_s^t \lambda(v) dv \Big) \Lambda_{x_1}(s,t) ds}{\exp\Big(\int_t^T \lambda(v) dv \Big)}
$$

$$
\begin{aligned}
f(t,T) &= f(0,T) + \gamma_1^2 \int_0^t \sigma^2(s)\exp\Big(- \int_s^T \lambda(v)dv \Big)\Lambda_{x_1}(s,T)ds + \gamma_1 \int_0^t \sigma(s)\exp\Big(- \int_s^T \lambda(v)dv \Big)dW(s) \\
&= f(0,T) + \exp\Big(- \int_t^T \lambda(v)dv \Big)y(t) + \gamma_1^2 \int_0^t \sigma^2(s)\exp\Big(- \int_s^T \lambda(v)dv \Big)\Lambda_{x_1}(s,T)ds \\
&- \gamma_1^2 \exp\Big(- \int_t^T \lambda(v)dv \Big) \int_0^t \sigma^2(s)\exp\Big(- \int_s^t \lambda(v)dv \Big)\Lambda_{x_1}(s,t)ds \\
&= f(0,T) + \exp\Big(- \int_t^T \lambda(v)dv \Big)y(t) + \gamma_1^2 \exp\Big(- \int_t^T \lambda(v)dv \Big) \\
&\times \int_0^t \sigma^2(s)\Big\{ \exp\Big(\int_t^T \lambda(v)dv \Big)\exp\Big(- \int_s^T \lambda(v)dv \Big)\Lambda_{x_1}(s,T) - \exp\Big(- \int_s^t \lambda(v)dv \Big)\Lambda_{x_1}(s,t) \Big\}ds \\
&= f(0,T) + \exp\Big(- \int_t^T \lambda(v)dv \Big)y(t) + \gamma_1^2 \exp\Big(- \int_t^T \lambda(v)dv \Big) \\
&\times \int_0^t \sigma^2(s)\exp\Big(- \int_s^t \lambda(v)dv \Big)\Big\{ \Lambda_{x_1}(s,T) - \Lambda_{x_1}(s,t) \Big\}ds \\
&= f(0,T) + \exp\Big(- \int_t^T \lambda(v)dv \Big)y(t) + \gamma_1^2 \Lambda(t,T)\exp\Big(- \int_t^T \lambda(v)dv \Big) \int_0^t \sigma^2(s)\exp\Big(- 2\int_s^t \lambda(v)dv \Big)ds \\
&= f(0,T) + \exp\Big(- \int_t^T \lambda(v)dv \Big)y(t) + \gamma_1^2 \Phi(t)\Lambda(t,T)\exp\Big(- \int_t^T \lambda(v)dv \Big)
\end{aligned}
$$

therefore:

$$
\begin{aligned}
\int_{x_1}^T f(t,u)du &= \int_{x_1}^T \Big(f(0,u) + \exp\Big(- \int_t^u \lambda(v)dv \Big)y(t) + \gamma_1^2 \Phi(t)\Lambda(t,u)\exp\Big(- \int_t^u \lambda(v)dv \Big) \Big)du \\
&= \int_{x_1}^T f(0,u)du + y(t) \int_{x_1}^T \exp\Big(- \int_t^u \lambda(v)dv \Big)du + \gamma_1^2 \Phi(t) \int_{x_1}^T \Lambda(t,u)\exp\Big(- \int_t^u \lambda(v)dv \Big)du \\
&= \int_{x_1}^T f(0,u)du + \Lambda_{x_1}(t,T)y(t) + \gamma_1^2 \Phi(t) \int_{x_1}^T \Lambda(t,u)d\Lambda(t,u) \\
&= \int_{x_1}^T f(0,u)du + \Lambda_{x_1}(t,T)y(t) + \frac{1}{2}\gamma_1^2 \Phi(t)\{\Lambda^2(t,T) - \Lambda^2(t,x_1)\}
\end{aligned}
$$

therefore:

$$
\int_t^{x_1} f(t,u)du + \int_{x_1}^T f(t,u)du = \int_t^T f(0,u)du + \Lambda_{x_1}(t,T)y(t) + \frac{1}{2}\gamma_1^2 \Phi(t)\{\Lambda^2(t,T) - \Lambda^2(t,x_1)\}
$$

Therefore, the bond price is given by

$$
B(t,T) = \exp\Big(- \int_t^T f(t,u)du \Big) = \frac{B(0,T)}{B(0,t)}\exp\Big(- \Lambda_{x_1}(t,T)y(t) - \frac{1}{2}\gamma_1^2 \Phi(t)\{\Lambda^2(t,T) - \Lambda^2(t,x_1)\} \Big) \tag{91}
$$

A.2.3 more general case $t < x_1 < T$

In general we will need $\int_{x_a}^{T} f(t,u)du$ where $T < x_{a+1}$, therefore restrict $T \in [x_a, x_{a+1}]$ and $t < x_1$, HJM result:

$$\begin{aligned}
f(t,T) &= f(0,T) + \int_0^t \sigma(s,T) \int_s^T \sigma(s,u)duds + \int_0^t \sigma(s,T)dW(s) \\
&= f(0,T) + \int_0^t \sum_{i=1}^{n} \mathbb{I}_{\{i \leq \mathcal{A}(s,T)\}} \chi(s)\phi(T)\gamma_i \int_s^T \sum_{j=1}^{n} \mathbb{I}_{\{j \leq \mathcal{A}(s,u)\}} \chi(s)\phi(u)\gamma_j duds \\
&+ \int_0^t \sum_{i=1}^{n} \mathbb{I}_{\{i \leq \mathcal{A}(s,T)\}} \chi(s)\phi(T)\gamma_i dW(s) \\
&= f(0,T) + \int_0^t \chi(s)\phi(T) \sum_{i=1}^{a} \gamma_i \int_s^T \sum_{j=1}^{n} \mathbb{I}_{\{j \leq \mathcal{A}(s,u)\}} \chi(s)\phi(u)\gamma_j duds + \int_0^t \chi(s)\phi(T) \sum_{i=1}^{a} \gamma_i dW(s)
\end{aligned}$$

Now

$$\int_s^T \sum_{j=1}^{n} \mathbb{I}_{\{j \leq \mathcal{A}(s,u)\}} \chi(s)\phi(u)\gamma_j du = \chi(s) \sum_{j=1}^{n} \gamma_j \int_s^T \mathbb{I}_{\{j \leq \mathcal{A}(s,u)\}} \phi(u)du \tag{92}$$

$$\begin{aligned}
\int_s^T \mathbb{I}_{\{j \leq \mathcal{A}(s,u)\}} \phi(u)du &= \int_s^{x_1} \mathbb{I}_{\{j \leq \mathcal{A}(s,u)\}} \phi(u)du + \sum_{k=1}^{a-1} \int_{x_k}^{x_{k+1}} \mathbb{I}_{\{j \leq \mathcal{A}(s,u)\}} \phi(u)du + \int_{x_a}^{T} \mathbb{I}_{\{j \leq \mathcal{A}(s,u)\}} \phi(u)du \\
&= \sum_{k=1}^{a-1} \int_{x_k}^{x_{k+1}} \mathbb{I}_{\{j \leq \mathcal{A}(s,u)\}} \phi(u)du + \int_{x_a}^{T} \mathbb{I}_{\{j \leq \mathcal{A}(s,u)\}} \phi(u)du
\end{aligned}$$

Therefore:

$$\begin{aligned}
\sum_{j=1}^{n} \gamma_j \int_s^T \mathbb{I}_{\{j \leq \mathcal{A}(s,u)\}} \phi(u)du &= \sum_{j=1}^{n} \gamma_j \sum_{k=1}^{a-1} \int_{x_k}^{x_{k+1}} \mathbb{I}_{\{j \leq \mathcal{A}(s,u)\}} \phi(u)du + \sum_{j=1}^{n} \gamma_j \int_{x_a}^{T} \mathbb{I}_{\{j \leq \mathcal{A}(s,u)\}} \phi(u)du \\
&= \sum_{j=1}^{a-1} \gamma_j \int_{x_j}^{x_a} \phi(u)du + \sum_{j=1}^{a} \gamma_j \int_{x_a}^{T} \phi(u)du \\
&= \sum_{j=1}^{a-1} \gamma_j \int_{x_j}^{T} \phi(u)du + \gamma_a \int_{x_a}^{T} \phi(u)du \\
&= \sum_{j=1}^{a} \gamma_j \int_{x_j}^{T} \phi(u)du
\end{aligned}$$

Therefore:

$$
\begin{aligned}
f(t,T) &= f(0,T) + \int_0^t \chi(s)\phi(T)\sum_{i=1}^{a}\gamma_i \int_s^T \sum_{j=1}^{n} \mathbb{I}_{\{j\le \mathcal{A}(s,u)\}}\chi(s)\phi(u)\gamma_j duds + \int_0^t \chi(s)\phi(T)\sum_{i=1}^{a}\gamma_i dW(s) \\
&= f(0,T) + \int_0^t \chi(s)\phi(T)\sum_{i=1}^{a}\gamma_i\chi(s)\sum_{j=1}^{a}\gamma_j \int_{x_j}^T \phi(u)duds + \int_0^t \chi(s)\phi(T)\sum_{i=1}^{a}\gamma_i dW(s) \\
&= f(0,T) + \sum_{i=1}^{a}\sum_{j=1}^{a}\gamma_i\gamma_j \int_0^t \chi(s)\phi(T)\int_{x_j}^T \chi(s)\phi(u)duds + \sum_{i=1}^{a}\gamma_i\int_0^t \chi(s)\phi(T)dW(s) \\
&= f(0,T) + \sum_{i=1}^{a}\sum_{j=1}^{a}\gamma_i\gamma_j \int_0^t \sigma(s)\exp\Big(\int_0^s \lambda(v)dv\Big)\exp\Big(-\int_0^T \lambda(v)dv\Big) \\
&\times \int_{x_j}^T \sigma(s)\exp\Big(\int_0^s \lambda(v)dv\Big)\exp\Big(-\int_0^u \lambda(v)dv\Big)duds \\
&+ \sum_{i=1}^{a}\gamma_i\int_0^t \sigma(s)\exp\Big(\int_0^s \lambda(v)dv\Big)\exp\Big(-\int_0^T \lambda(v)dv\Big)dW(s) \\
&= f(0,T) + \sum_{i=1}^{a}\sum_{j=1}^{a}\gamma_i\gamma_j \int_0^t \sigma^2(s)\exp\Big(-\int_s^T \lambda(v)dv\Big)\int_{x_j}^T \exp\Big(-\int_s^u \lambda(v)dv\Big)duds \\
&+ \sum_{i=1}^{a}\gamma_i\int_0^t \sigma(s)\exp\Big(-\int_s^T \lambda(v)dv\Big)dW(s) \\
&= f(0,T) + \sum_{i=1}^{a}\sum_{j=1}^{a}\gamma_i\gamma_j \int_0^t \sigma^2(s)\exp\Big(-\int_s^T \lambda(v)dv\Big)\Lambda_{x_j}(s,T)ds \\
&+ \sum_{i=1}^{a}\gamma_i\int_0^t \sigma(s)\exp\Big(-\int_s^T \lambda(v)dv\Big)dW(s)
\end{aligned}
$$

Let

$$
\begin{aligned}
y_a(t) = &\sum_{i=1}^{a}\sum_{j=1}^{a}\gamma_i\gamma_j \int_0^t \sigma^2(s)\exp\Big(-\int_s^t \lambda(v)dv\Big)\Lambda_{x_j}(s,t)ds \\
&+ \exp\Big(\int_t^T \lambda(v)dv\Big)\sum_{i=1}^{a}\gamma_i\int_0^t \sigma(s)\exp\Big(-\int_s^T \lambda(v)dv\Big)dW(s)
\end{aligned}
$$

Substitute

$$
\sum_{i=1}^{a}\gamma_i\int_0^t \sigma(s)\exp\Big(-\int_s^T \lambda(v)dv\Big)dW(s) = \frac{y_a(t) - \sum_{i=1}^{a}\sum_{j=1}^{a}\gamma_i\gamma_j\int_0^t \sigma^2(s)\exp\Big(-\int_s^t \lambda(v)dv\Big)\Lambda_{x_j}(s,t)ds}{\exp\Big(\int_t^T \lambda(v)dv\Big)}
$$

$$
\begin{aligned}
f(t,T) &= f(0,T) + \sum_{i=1}^{a}\sum_{j=1}^{a}\gamma_i\gamma_j\int_0^t \sigma^2(s)\exp\Big(-\int_s^T \lambda(v)dv\Big)\Lambda_{x_j}(s,T)ds \\
&+ \sum_{i=1}^{a}\gamma_i\int_0^t \sigma(s)\exp\Big(-\int_s^T \lambda(v)dv\Big)dW(s) \\
&= f(0,T) + \exp\Big(-\int_t^T \lambda(v)dv\Big)y_a(t) + \sum_{i=1}^{a}\sum_{j=1}^{a}\gamma_i\gamma_j\int_0^t \sigma^2(s)\exp\Big(-\int_s^T \lambda(v)dv\Big)\Lambda_{x_j}(s,T)ds \\
&- \sum_{i=1}^{a}\sum_{j=1}^{a}\gamma_i\gamma_j\exp\Big(-\int_t^T \lambda(v)dv\Big)\int_0^t \sigma^2(s)\exp\Big(-\int_s^t \lambda(v)dv\Big)\Lambda_{x_j}(s,t)ds \\
&= f(0,T) + \exp\Big(-\int_t^T \lambda(v)dv\Big)y(t) + \sum_{i=1}^{a}\sum_{j=1}^{a}\gamma_i\gamma_j\exp\Big(-\int_t^T \lambda(v)dv\Big) \\
&\times \int_0^t \sigma^2(s)\Big\{\exp\Big(\int_t^T \lambda(v)dv\Big)\exp\Big(-\int_s^T \lambda(v)dv\Big)\Lambda_{x_j}(s,T) - \exp\Big(-\int_s^t \lambda(v)dv\Big)\Lambda_{x_j}(s,t)\Big\}ds \\
&= f(0,T) + \exp\Big(-\int_t^T \lambda(v)dv\Big)y_a(t) + \sum_{i=1}^{a}\sum_{j=1}^{a}\gamma_i\gamma_j\exp\Big(-\int_t^T \lambda(v)dv\Big) \\
&\times \int_0^t \sigma^2(s)\exp\Big(-\int_s^t \lambda(v)dv\Big)\Big\{\Lambda_{x_j}(s,T) - \Lambda_{x_j}(s,t)\Big\}ds \\
&= f(0,T) + \exp\Big(-\int_t^T \lambda(v)dv\Big)y_a(t) \\
&+ \sum_{i=1}^{a}\sum_{j=1}^{a}\gamma_i\gamma_j\Lambda(t,T)\exp\Big(-\int_t^T \lambda(v)dv\Big)\int_0^t \sigma^2(s)\exp\Big(-2\int_s^t \lambda(v)dv\Big)ds \\
&= f(0,T) + \exp\Big(-\int_t^T \lambda(v)dv\Big)y_a(t) + \sum_{i=1}^{a}\sum_{j=1}^{a}\gamma_i\gamma_j\Phi(t)\Lambda(t,T)\exp\Big(-\int_t^T \lambda(v)dv\Big)
\end{aligned}
$$

Therefore:

$$
\begin{aligned}
\int_{x_a}^T f(t,u)du &= \int_{x_a}^T \Big(f(0,u) + \exp\Big(-\int_t^u \lambda(v)dv\Big)y_a(t) + \sum_{i=1}^{a}\sum_{j=1}^{a}\gamma_i\gamma_j\Phi(t)\Lambda(t,u)\exp\Big(-\int_t^u \lambda(v)dv\Big)\Big)du \\
&= \int_{x_a}^T f(0,u)du + y_a(t)\int_{x_a}^T \exp\Big(-\int_t^u \lambda(v)dv\Big)du \\
&+ \sum_{i=1}^{a}\sum_{j=1}^{a}\gamma_i\gamma_j\Phi(t)\int_{x_a}^T \Lambda(t,u)\exp\Big(-\int_t^u \lambda(v)dv\Big)du \\
&= \int_{x_a}^T f(0,u)du + \Lambda_{x_a}(t,T)y_a(t) + \sum_{i=1}^{a}\sum_{j=1}^{a}\gamma_i\gamma_j\Phi(t)\int_{x_a}^T \Lambda(t,u)d\Lambda(t,u) \\
&= \int_{x_a}^T f(0,u)du + \Lambda_{x_a}(t,T)y_a(t) + \frac{1}{2}\sum_{i=1}^{a}\sum_{j=1}^{a}\gamma_i\gamma_j\Phi(t)\{\Lambda^2(t,T) - \Lambda^2(t,x_a)\}
\end{aligned}
$$

Define $\eta(t) = \min\{k|x_k > t\}$, now:

$$\begin{aligned}\int_t^T f(t,u)du &= \int_t^{x_{\eta(t)}} f(t,u)du + \int_{x_{\eta(T)-1}}^T f(t,u)du + \sum_{k=\eta(t)}^{\eta(T)-2}\int_{x_k}^{x_{k+1}} f(t,u)du \\ &= \int_t^T f(0,u)du + \Lambda_{x_{\eta(T)-1}}(t,T)y_{x_{\eta(T)-1}}(t) \\ &+ \frac{1}{2}\sum_{i=1}^{x_{\eta(T)-1}}\sum_{j=1}^{x_{\eta(T)-1}} \gamma_i\gamma_j\Phi(t)\{\Lambda^2(t,T) - \Lambda^2(t,x_{\eta(T)-1})\} \\ &+ \sum_{k=\eta(t)}^{\eta(T)-2}\left(\Lambda_{x_k}(t,x_{k+1})y_k(t) + \frac{1}{2}\sum_{i=1}^{k}\sum_{j=1}^{k}\gamma_i\gamma_j\Phi(t)\{\Lambda^2(t,x_{k+1}) - \Lambda^2(t,x_k)\}\right)\end{aligned}$$

Therefore, the bond price is given by

$$\begin{aligned}B(t,T) &= \exp\Big(-\int_t^T f(t,u)du\Big) \\ &= \frac{B(0,T)}{B(0,t)}\exp\Bigg(\Lambda_{x_{\eta(T)-1}}(t,T)y_{x_{\eta(T)-1}}(t) + \frac{1}{2}\sum_{i=1}^{x_{\eta(T)-1}}\sum_{j=1}^{x_{\eta(T)-1}}\gamma_i\gamma_j\Phi(t)\{\Lambda^2(t,T) - \Lambda^2(t,x_{\eta(T)-1})\} \\ &+ \sum_{k=\eta(t)}^{\eta(T)-2}\left(\Lambda_{x_k}(t,x_{k+1})y_k(t) + \frac{1}{2}\sum_{i=1}^{k}\sum_{j=1}^{k}\gamma_i\gamma_j\Phi(t)\{\Lambda^2(t,x_{k+1}) - \Lambda^2(t,x_k)\}\right)\Bigg)\end{aligned}$$

A.2.4 general case $t < T$

In general we will need $\int_{x_a}^T f(t,u)du$ where $T < x_{a+1}$, therefore restrict $T \in [x_a, x_{a+1}]$ and $t < T$. Define $\eta(t) = \min\{b|x_b \geq t\}$, now HJM result:

$$\begin{aligned}f(t,T) &= f(0,T) + \int_0^t \sigma(s,T)\int_s^T \sigma(s,u)duds + \int_0^t \sigma(s,T)dW(s) \\ &= f(0,T) + \int_{x_{\eta(t)-1}}^t \sigma(s,T)\int_s^T \sigma(s,u)duds + \sum_{b=0}^{\eta(t)-2}\int_{x_b}^{x_{b+1}} \sigma(s,T)\int_s^T \sigma(s,u)duds \\ &+ \int_{x_{\eta(t)-1}}^t \sigma(s,T)dW(s) + \sum_{b=0}^{\eta(t)-2}\int_{x_b}^{x_{b+1}} \sigma(s,T)dW(s) \qquad (93)\end{aligned}$$

Therefore, in general we need to solve $\int_{x_b}^{t}\sigma(s,T)\int_{s}^{T}\sigma(s,u)duds$ and $\int_{x_b}^{t}\sigma(s,T)dW(s)$ where $t\in[x_b,x_{b+1}]$. Now:

$$\begin{aligned}\int_{x_b}^{t}\sigma(s,T)dW(s) &= \int_{x_b}^{t}\sum_{i=1}^{n}\mathbb{I}_{\{i\leq\mathcal{A}(s,T)\}}\chi(s)\phi(T)\gamma_i dW(s)\\ &= \int_{x_b}^{t}\chi(s)\phi(T)\sum_{i=1}^{a-b}\gamma_i dW(s)\\ &= \sum_{i=1}^{a-b}\gamma_i\int_{x_b}^{t}\sigma(s)\exp\Big(\int_0^s\lambda(v)dv\Big)\exp\Big(-\int_0^T\lambda(v)dv\Big)dW(s)\\ &= \sum_{i=1}^{a-b}\gamma_i\int_{x_b}^{t}\sigma(s)\exp\Big(-\int_s^T\lambda(v)dv\Big)dW(s)\end{aligned}$$

Also:

$$\begin{aligned}\int_{x_b}^{t}\sigma(s,T)\int_{s}^{T}\sigma(s,u)duds &= \int_{x_b}^{t}\sum_{i=1}^{n}\mathbb{I}_{\{i\leq\mathcal{A}(s,T)\}}\chi(s)\phi(T)\gamma_i\int_{s}^{T}\sum_{j=1}^{n}\mathbb{I}_{\{j\leq\mathcal{A}(s,u)\}}\chi(s)\phi(u)\gamma_j duds\\ &= \int_{x_b}^{t}\chi(s)\phi(T)\sum_{i=1}^{a-b}\gamma_i\int_{s}^{T}\sum_{j=1}^{n}\mathbb{I}_{\{j\leq\mathcal{A}(s,u)\}}\chi(s)\phi(u)\gamma_j duds\\ &= \int_{x_b}^{t}\chi(s)\phi(T)\sum_{i=1}^{a-b}\gamma_i\chi(s)\sum_{j=1}^{n}\gamma_j\int_{s}^{T}\mathbb{I}_{\{j\leq\mathcal{A}(s,u)\}}\phi(u)duds\end{aligned}$$

Now, implicitly with $s\in[x_b,t]$:

$$\begin{aligned}\int_{s}^{T}\mathbb{I}_{\{j\leq\mathcal{A}(s,u)\}}\phi(u)du &= \int_{s}^{x_1}\mathbb{I}_{\{j\leq\mathcal{A}(s,u)\}}\phi(u)du+\sum_{k=1}^{a-1}\int_{x_k}^{x_{k+1}}\mathbb{I}_{\{j\leq\mathcal{A}(s,u)\}}\phi(u)du+\int_{x_a}^{T}\mathbb{I}_{\{j\leq\mathcal{A}(s,u)\}}\phi(u)du\\ &= \sum_{k=b+1}^{a-1}\int_{x_k}^{x_{k+1}}\mathbb{I}_{\{j\leq\mathcal{A}(s,u)\}}\phi(u)du+\int_{x_a}^{T}\mathbb{I}_{\{j\leq\mathcal{A}(s,u)\}}\phi(u)du\end{aligned}$$

Therefore:

$$\begin{aligned}\sum_{j=1}^{n}\gamma_j\int_{s}^{T}\mathbb{I}_{\{j\leq\mathcal{A}(s,u)\}}\phi(u)du &= \sum_{j=1}^{n}\gamma_j\sum_{k=b+1}^{a-1}\int_{x_k}^{x_{k+1}}\mathbb{I}_{\{j\leq\mathcal{A}(s,u)\}}\phi(u)du+\sum_{j=1}^{n}\gamma_j\int_{x_a}^{T}\mathbb{I}_{\{j\leq\mathcal{A}(s,u)\}}\phi(u)du\\ &= \sum_{j=1}^{a-b-1}\gamma_j\int_{x_{b+j}}^{x_a}\phi(u)du+\sum_{j=1}^{a-b}\gamma_j\int_{x_a}^{T}\phi(u)du\\ &= \sum_{j=1}^{a-b-1}\gamma_j\int_{x_{b+j}}^{T}\phi(u)du+\gamma_{a-b}\int_{x_a}^{T}\phi(u)du\\ &= \sum_{j=1}^{a-b}\gamma_j\int_{x_{b+j}}^{T}\phi(u)du\end{aligned}$$

Therefore:

$$\int_{x_b}^{t}\sigma(s,T)\int_{s}^{T}\sigma(s,u)duds=\int_{x_b}^{t}\chi(s)\phi(T)\sum_{i=1}^{a-b}\gamma_i\chi(s)\sum_{j=1}^{n}\gamma_j\int_{s}^{T}\mathbb{I}_{\{j\leq\mathcal{A}(s,u)\}}\phi(u)duds$$

$$=\int_{x_b}^{t}\chi(s)\phi(T)\sum_{i=1}^{a-b}\gamma_i\sum_{j=1}^{a-b}\gamma_j\int_{x_{b+j}}^{T}\chi(s)\phi(u)duds$$

$$=\sum_{i=1}^{a-b}\sum_{j=1}^{a-b}\gamma_i\gamma_j\int_{x_b}^{t}\chi(s)\phi(T)\int_{x_{b+j}}^{T}\chi(s)\phi(u)duds$$

$$=\sum_{i=1}^{a-b}\sum_{j=1}^{a-b}\gamma_i\gamma_j\int_{x_b}^{t}\sigma(s)\exp\Big(\int_0^s\lambda(v)dv\Big)\exp\Big(-\int_0^T\lambda(v)dv\Big)$$

$$\times\int_{x_{b+j}}^{T}\sigma(s)\exp\Big(\int_0^s\lambda(v)dv\Big)\exp\Big(-\int_0^u\lambda(v)dv\Big)duds$$

$$=\sum_{i=1}^{a-b}\sum_{j=1}^{a-b}\gamma_i\gamma_j\int_{x_b}^{t}\sigma^2(s)\exp\Big(-\int_s^T\lambda(v)dv\Big)\int_{x_{b+j}}^{T}\exp\Big(-\int_s^u\lambda(v)dv\Big)duds$$

$$=\sum_{i=1}^{a-b}\sum_{j=1}^{a-b}\gamma_i\gamma_j\int_{x_b}^{t}\sigma^2(s)\exp\Big(-\int_s^T\lambda(v)dv\Big)\Lambda_{x_{b+j}}(s,T)ds$$

Rewrite (93):

$$f(t,T)=f(0,T)+\int_0^t\sigma(s,T)\int_s^T\sigma(s,u)duds+\int_0^t\sigma(s,T)dW(s)$$

$$=f(0,T)+\sum_{b=0}^{\eta(t)-2}\Big\{\int_{x_b}^{x_{b+1}}\sigma(s,T)\int_s^T\sigma(s,u)duds+\int_{x_b}^{x_{b+1}}\sigma(s,T)dW(s)\Big\}$$

$$+\int_{x_{\eta(t)-1}}^{t}\sigma(s,T)\int_s^T\sigma(s,u)duds+\int_{x_{\eta(t)-1}}^{t}\sigma(s,T)dW(s)$$

$$=f(0,T)+\sum_{b=0}^{\eta(t)-2}\Big\{\sum_{i=1}^{a-b}\sum_{j=1}^{a-b}\gamma_i\gamma_j\int_{x_b}^{x_{b+1}}\sigma^2(s)\exp\Big(-\int_s^T\lambda(v)dv\Big)\Lambda_{x_{b+j}}(s,T)ds$$

$$+\sum_{i=1}^{a-b}\gamma_i\int_{x_b}^{x_{b+1}}\sigma(s)\exp\Big(-\int_s^T\lambda(v)dv\Big)dW(s)\Big\}$$

$$+\sum_{i=1}^{(a-\eta(t)+1)}\sum_{j=1}^{(a-\eta(t)+1)}\gamma_i\gamma_j\int_{x_{\eta(t)-1}}^{t}\sigma^2(s)\exp\Big(-\int_s^T\lambda(v)dv\Big)\Lambda_{x_{(\eta(t)-1+j)}}(s,T)ds$$

$$+\sum_{i=1}^{a-\eta(t)+1}\gamma_i\int_{x_{\eta(t)-1}}^{t}\sigma(s)\exp\Big(-\int_s^T\lambda(v)dv\Big)dW(s)$$

Let

$$y_a(t) = \sum_{i=1}^{(a-\eta(t)+1)} \sum_{j=1}^{(a-\eta(t)+1)} \gamma_i\gamma_j \int_{x_{\eta(t)-1}}^{t} \sigma^2(s)\exp\Big(- \int_s^t \lambda(v)dv\Big)\Lambda_{x_{(\eta(t)-1+j)}}(s,t)ds$$
$$+ \exp\Big(\int_t^T \lambda(v)dv\Big) \sum_{i=1}^{a-\eta(t)+1} \gamma_i \int_{x_{\eta(t)-1}}^{t} \sigma(s)\exp\Big(- \int_s^T \lambda(v)dv\Big)dW(s)$$

Substitute

$$\sum_{i=1}^{a-\eta(t)+1} \gamma_i \int_{x_{\eta(t)-1}}^{t} \sigma(s)\exp\Big(- \int_s^T \lambda(v)dv\Big)dW(s)$$
$$= \frac{y_a(t) - \sum_{i=1}^{(a-\eta(t)+1)} \sum_{j=1}^{(a-\eta(t)+1)} \gamma_i\gamma_j \int_{x_{\eta(t)-1}}^{t} \sigma^2(s)\exp\Big(- \int_s^t \lambda(v)dv\Big)\Lambda_{x_{(\eta(t)-1+j)}}(s,t)ds}{\exp\Big(\int_t^T \lambda(v)dv\Big)}$$

Define

$$\Phi(u,t) = \int_u^t \sigma^2(s)\exp\Big(- 2\int_s^t \lambda(v)dv\Big)ds \tag{94}$$

Therefore

$$\sum_{i=1}^{a-b} \sum_{j=1}^{a-b} \gamma_i\gamma_j \int_{x_b}^{x_{b+1}} \sigma^2(s)\exp\Big(- \int_s^T \lambda(v)dv\Big)\Lambda_{x_{b+j}}(s,T)ds + \sum_{i=1}^{a-b} \gamma_i \int_{x_b}^{x_{b+1}} \sigma(s)\exp\Big(- \int_s^T \lambda(v)dv\Big)dW(s)$$
$$= \exp\Big(- \int_{x_{b+1}}^T \lambda(v)dv\Big)y_a(x_{b+1}) + \sum_{i=1}^{a-b} \sum_{j=1}^{a-b} \gamma_i\gamma_j \int_{x_b}^{x_{b+1}} \sigma^2(s)\exp\Big(- \int_s^T \lambda(v)dv\Big)\Lambda_{x_{b+j}}(s,T)ds$$
$$- \sum_{i=1}^{a-b} \sum_{j=1}^{a-b} \gamma_i\gamma_j \exp\Big(- \int_{x_{b+1}}^T \lambda(v)dv\Big) \int_{x_b}^{x_{b+1}} \sigma^2(s)\exp\Big(- \int_s^{x_{b+1}} \lambda(v)dv\Big)\Lambda_{x_{b+j}}(s,x_{b+1})ds$$
$$= \exp\Big(- \int_{x_{b+1}}^T \lambda(v)dv\Big)y_a(x_{b+1}) + \sum_{i=1}^{a-b} \sum_{j=1}^{a-b} \Big\{ \gamma_i\gamma_j \exp\Big(- \int_{x_{b+1}}^T \lambda(v)dv\Big)$$
$$\times \Big[\int_{x_b}^{x_{b+1}} \sigma^2(s)\Big\{ \exp\Big(\int_{x_{b+1}}^T \lambda(v)dv\Big)\exp\Big(- \int_s^T \lambda(v)dv\Big)\Lambda_{x_{b+j}}(s,T)$$
$$- \exp\Big(- \int_s^{x_{b+1}} \lambda(v)dv\Big)\Lambda_{x_{b+j}}(s,x_{b+1})\Big\}ds\Big]\Big\}$$
$$= \exp\Big(- \int_{x_{b+1}}^T \lambda(v)dv\Big)y_a(x_{b+1}) + \sum_{i=1}^{a-b} \sum_{j=1}^{a-b} \gamma_i\gamma_j\Lambda(x_{b+1},T)\exp\Big(- \int_{x_{b+1}}^T \lambda(v)dv\Big)$$
$$\times \int_{x_b}^{x_{b+1}} \sigma^2(s)\exp\Big(- 2\int_s^{x_{b+1}} \lambda(v)dv\Big)ds$$
$$= \exp\Big(- \int_{x_{b+1}}^T \lambda(v)dv\Big)y_a(x_{b+1}) + \sum_{i=1}^{a-b} \sum_{j=1}^{a-b} \gamma_i\gamma_j\Phi(x_b,x_{b+1})\Lambda(x_{b+1},T)\exp\Big(- \int_{x_{b+1}}^T \lambda(v)dv\Big)$$

and

$$\sum_{i=1}^{(a-\eta(t)+1)}\sum_{j=1}^{(a-\eta(t)+1)}\gamma_i\gamma_j\int_{x_{\eta(t)-1}}^{t}\sigma^2(s)\exp\Big(-\int_s^T\lambda(v)dv\Big)\Lambda_{x_{(\eta(t)-1+j)}}(s,T)ds$$

$$+\sum_{i=1}^{a-\eta(t)+1}\gamma_i\int_{x_{\eta(t)+1}}^{t}\sigma(s)\exp\Big(-\int_s^T\lambda(v)dv\Big)dW(s)$$

$$=\exp\Big(-\int_t^T\lambda(v)dv\Big)y_a(t)+\sum_{i=1}^{(a-\eta(t)+1)}\sum_{j=1}^{(a-\eta(t)+1)}\gamma_i\gamma_j\int_{x_{\eta(t)-1}}^{t}\sigma^2(s)\exp\Big(-\int_s^T\lambda(v)dv\Big)\Lambda_{x_{(\eta(t)-1+j)}}(s,T)ds$$

$$-\sum_{i=1}^{(a-\eta(t)+1)}\sum_{j=1}^{(a-\eta(t)+1)}\gamma_i\gamma_j\exp\Big(-\int_t^T\lambda(v)dv\Big)\int_{x_{\eta(t)-1}}^{t}\sigma^2(s)\exp\Big(-\int_s^T\lambda(v)dv\Big)\Lambda_{x_{(\eta(t)-1+j)}}(s,t)ds$$

$$=\exp\Big(-\int_t^T\lambda(v)dv\Big)y_a(t)+\sum_{i=1}^{(a-\eta(t)+1)}\sum_{j=1}^{(a-\eta(t)+1)}\Big\{\gamma_i\gamma_j\exp\Big(-\int_t^T\lambda(v)dv\Big)$$

$$\times\Big[\int_{x_{\eta(t)-1}}^{t}\sigma^2(s)\Big\{\exp\Big(\int_t^T\lambda(v)dv\Big)\exp\Big(-\int_s^T\lambda(v)dv\Big)\Lambda_{x_{(\eta(t)-1+j)}}(s,T)$$

$$-\exp\Big(-\int_s^t\lambda(v)dv\Big)\Lambda_{x_{(\eta(t)-1+j)}}(s,t)\Big\}ds\Big]\Big\}$$

$$=\exp\Big(-\int_t^T\lambda(v)dv\Big)y_a(t)+\sum_{i=1}^{(a-\eta(t)+1)}\sum_{j=1}^{(a-\eta(t)+1)}\gamma_i\gamma_j\Lambda(t,T)\exp\Big(-\int_t^T\lambda(v)dv\Big)$$

$$\times\int_{x_{\eta(t)-1}}^{t}\sigma^2(s)\exp\Big(-2\int_s^t\lambda(v)dv\Big)ds$$

$$=\exp\Big(-\int_t^T\lambda(v)dv\Big)y_a(t)+\sum_{i=1}^{(a-\eta(t)+1)}\sum_{j=1}^{(a-\eta(t)+1)}\gamma_i\gamma_j\Phi(x_{\eta(t)-1},t)\Lambda(t,T)\exp\Big(-\int_t^T\lambda(v)dv\Big)$$

Therefore:

$$
\begin{aligned}
f(t,T) &= f(0,T) + \sum_{b=0}^{\eta(t)-2} \Bigg\{ \sum_{i=1}^{a-b}\sum_{j=1}^{a-b} \gamma_i\gamma_j \int_{x_b}^{x_{b+1}} \sigma^2(s)\exp\Big(-\int_s^T \lambda(v)dv \Big)\Lambda_{x_{b+j}}(s,T)ds \\
&+ \sum_{i=1}^{a-b} \gamma_i \int_{x_b}^{x_{b+1}} \sigma(s)\exp\Big(-\int_s^T \lambda(v)dv \Big) dW(s) \Bigg\} \\
&+ \sum_{i=1}^{(a-\eta(t)+1)} \sum_{j=1}^{(a-\eta(t)+1)} \gamma_i\gamma_j \int_{x_{\eta(t)-1}}^{t} \sigma^2(s)\exp\Big(-\int_s^T \lambda(v)dv \Big)\Lambda_{x_{(\eta(t)-1+j)}}(s,T)ds \\
&+ \sum_{i=1}^{a-\eta(t)+1} \gamma_i \int_{x_{\eta(t)-1}}^{t} \sigma(s)\exp\Big(-\int_s^T \lambda(v)dv \Big) dW(s) \\
&= f(0,T) + \sum_{b=0}^{\eta(t)-2} \Bigg\{ \exp\Big(-\int_{x_{b+1}}^T \lambda(v)dv \Big) y_a(x_{b+1}) \\
&+ \sum_{i=1}^{a-b}\sum_{j=1}^{a-b} \gamma_i\gamma_j \Phi(x_b, x_{b+1})\Lambda(x_{b+1},T)\exp\Big(-\int_{x_{b+1}}^T \lambda(v)dv \Big) \Bigg\} \\
&+ \exp\Big(-\int_t^T \lambda(v)dv \Big) y_a(t) + \sum_{i=1}^{(a-\eta(t)+1)} \sum_{j=1}^{(a-\eta(t)+1)} \gamma_i\gamma_j \Phi(x_{\eta(t)-1}, t)\Lambda(t,T)\exp\Big(-\int_t^T \lambda(v)dv \Big) \\
&= f(0,T) + \sum_{b=0}^{\eta(t)-2} \exp\Big(-\int_{x_{b+1}}^T \lambda(v)dv \Big) y_a(x_{b+1}) + \exp\Big(-\int_t^T \lambda(v)dv \Big) y_a(t) \\
&+ \sum_{b=0}^{\eta(t)-2} \sum_{i=1}^{a-b}\sum_{j=1}^{a-b} \gamma_i\gamma_j \Phi(x_b, x_{b+1})\Lambda(x_{b+1},T)\exp\Big(-\int_{x_{b+1}}^T \lambda(v)dv \Big) \\
&+ \sum_{i=1}^{(a-\eta(t)+1)} \sum_{j=1}^{(a-\eta(t)+1)} \gamma_i\gamma_j \Phi(x_{\eta(t)-1}, t)\Lambda(t,T)\exp\Big(-\int_t^T \lambda(v)dv \Big)
\end{aligned}
$$

Therefore:

$$\int_{x_a}^{T} f(t,u)du = \int_{x_a}^{T} \Bigg(f(0,u) + \sum_{b=0}^{\eta(t)-2} \exp\Big(-\int_{x_{b+1}}^{u} \lambda(v)dv \Big) y_a(x_{b+1}) + \exp\Big(-\int_{t}^{u} \lambda(v)dv \Big) y_a(t)$$

$$+ \sum_{b=0}^{\eta(t)-2} \sum_{i=1}^{a-b} \sum_{j=1}^{a-b} \gamma_i \gamma_j \Phi(x_b, x_{b+1}) \Lambda(x_{b+1}, u) \exp\Big(-\int_{x_{b+1}}^{u} \lambda(v)dv \Big)$$

$$+ \sum_{i=1}^{(a-\eta(t)+1)} \sum_{j=1}^{(a-\eta(t)+1)} \gamma_i \gamma_j \Phi(x_{\eta(t)-1}, t) \Lambda(t,u) \exp\Big(-\int_{t}^{u} \lambda(v)dv \Big) \Bigg) du$$

$$= \int_{x_a}^{T} f(0,u)du + \sum_{b=0}^{\eta(t)-2} y_a(x_{b+1}) \int_{x_a}^{T} \exp\Big(-\int_{x_{b+1}}^{u} \lambda(v)dv \Big) du + y_a(t) \int_{x_a}^{T} \exp\Big(-\int_{t}^{u} \lambda(v)dv \Big) du$$

$$+ \sum_{b=0}^{\eta(t)-2} \sum_{i=1}^{a-b} \sum_{j=1}^{a-b} \gamma_i \gamma_j \Phi(x_b, x_{b+1}) \int_{x_a}^{T} \Lambda(x_{b+1}, u) \exp\Big(-\int_{x_{b+1}}^{u} \lambda(v)dv \Big) du$$

$$+ \sum_{i=1}^{(a-\eta(t)+1)} \sum_{j=1}^{(a-\eta(t)+1)} \gamma_i \gamma_j \Phi(x_{\eta(t)-1}, t) \int_{x_a}^{T} \Lambda(t,u) \exp\Big(-\int_{t}^{u} \lambda(v)dv \Big) du$$

$$= \int_{x_a}^{T} f(0,u)du + \sum_{b=0}^{\eta(t)-2} \Lambda_{x_a}(x_{b+1}, T) y_a(x_{b+1}) + \Lambda_{x_a}(t,T) y_a(t)$$

$$+ \sum_{b=0}^{\eta(t)-2} \sum_{i=1}^{a-b} \sum_{j=1}^{a-b} \gamma_i \gamma_j \Phi(x_b, x_{b+1}) \int_{x_a}^{T} \Lambda(x_{b+1}, u) d\Lambda(x_{b+1}, u)$$

$$+ \sum_{i=1}^{(a-\eta(t)+1)} \sum_{j=1}^{(a-\eta(t)+1)} \gamma_i \gamma_j \Phi(x_{\eta(t)-1}, t) \int_{x_a}^{T} \Lambda(t,u) d\Lambda(t,u)$$

$$= \int_{x_a}^{T} f(0,u)du + \sum_{b=0}^{\eta(t)-2} \Lambda_{x_a}(x_{b+1}, T) y_a(x_{b+1}) + \Lambda_{x_a}(t,T) y_a(t)$$

$$+ \frac{1}{2} \sum_{b=0}^{\eta(t)-2} \sum_{i=1}^{a-b} \sum_{j=1}^{a-b} \gamma_i \gamma_j \Phi(x_b, x_{b+1}) \{ \Lambda^2(x_{b+1}, T) - \Lambda^2(x_{b+1}, x_a) \}$$

$$+ \frac{1}{2} \sum_{i=1}^{(a-\eta(t)+1)} \sum_{j=1}^{(a-\eta(t)+1)} \gamma_i \gamma_j \Phi(x_{\eta(t)-1}, t) \{ \Lambda^2(t,T) - \Lambda^2(t, x_a) \}$$

Now

$$\int_t^T f(t,u)du = \int_t^{x_{\eta(t)}} f(t,u)du + \int_{x_{\eta(T)-1}}^T f(t,u)du + \sum_{k=\eta(t)}^{\eta(T)-2} \int_{x_k}^{x_{k+1}} f(t,u)du$$

$$= \int_t^T f(0,u)du + \sum_{b=0}^{\eta(t)-2} \Lambda_{x_{\eta(T)-1}}(x_{b+1},T)y_{\eta(T)-1}(x_{b+1}) + \Lambda_{x_{\eta(T)-1}}(t,T)y_{\eta(T)-1}(t)$$
$$+ \frac{1}{2}\sum_{b=0}^{\eta(t)-2}\sum_{i=1}^{\eta(T)-1-b}\sum_{j=1}^{\eta(T)-1-b} \gamma_i\gamma_j\Phi(x_b,x_{b+1})\{\Lambda^2(x_{b+1},T) - \Lambda^2(x_{b+1},x_{\eta(T)-1})\}$$
$$+ \frac{1}{2}\sum_{i=1}^{\eta(T)-\eta(t)}\sum_{j=1}^{\eta(T)-\eta(t)} \gamma_i\gamma_j\Phi(x_{\eta(t)-1},t)\{\Lambda^2(t,T) - \Lambda^2(t,x_{\eta(T)-1})\}$$
$$+ \sum_{k=\eta(t)}^{\eta(T)-2}\Bigg[\sum_{b=0}^{\eta(t)-2} \Lambda_{x_k}(x_{b+1},x_{k+1})y_k(x_{b+1}) + \Lambda_{x_k}(t,x_{k+1})y_k(t)$$
$$+ \frac{1}{2}\sum_{b=0}^{\eta(t)-2}\sum_{i=1}^{k-b}\sum_{j=1}^{k-b}\gamma_i\gamma_j\Phi(x_b,x_{b+1})\{\Lambda^2(x_{b+1},x_{k+1}) - \Lambda^2(x_{b+1},x_k)\}$$
$$+ \frac{1}{2}\sum_{i=1}^{(k-\eta(t)+1)}\sum_{j=1}^{(a-\eta(t)+1)} \gamma_i\gamma_j\Phi(x_{\eta(t)-1},t)\{\Lambda^2(t,x_{k+1}) - \Lambda^2(t,x_k)\}\Bigg]$$

$$= \int_t^T f(0,u)du$$
$$+ \sum_{b=0}^{\eta(t)-2} \Lambda_{x_{\eta(T)-1}}(x_{b+1},T)y_{\eta(T)-1}(x_{b+1})$$
$$+ \Lambda_{x_{\eta(T)-1}}(t,T)y_{\eta(T)-1}(t)$$
$$+ \sum_{k=\eta(t)}^{\eta(T)-2}\sum_{b=0}^{\eta(t)-2} \Lambda_{x_k}(x_{b+1},x_{k+1})y_k(x_{b+1})$$
$$+ \sum_{k=\eta(t)}^{\eta(T)-2} \Lambda_{x_k}(t,x_{k+1})y_k(t)$$
$$+ \frac{1}{2}\sum_{b=0}^{\eta(t)-2}\sum_{i=1}^{\eta(T)-1-b}\sum_{j=1}^{\eta(T)-1-b} \gamma_i\gamma_j\Phi(x_b,x_{b+1})\{\Lambda^2(x_{b+1},T) - \Lambda^2(x_{b+1},x_{\eta(T)-1})\}$$
$$+ \frac{1}{2}\sum_{i=1}^{\eta(T)-\eta(t)}\sum_{j=1}^{\eta(T)-\eta(t)} \gamma_i\gamma_j\Phi(x_{\eta(t)-1},t)\{\Lambda^2(t,T) - \Lambda^2(t,x_{\eta(T)-1})\}$$
$$+ \sum_{k=\eta(t)}^{\eta(T)-2}\frac{1}{2}\sum_{b=0}^{\eta(t)-2}\sum_{i=1}^{k-b}\sum_{j=1}^{k-b}\gamma_i\gamma_j\Phi(x_b,x_{b+1})\{\Lambda^2(x_{b+1},x_{k+1}) - \Lambda^2(x_{b+1},x_k)\}$$
$$+ \sum_{k=\eta(t)}^{\eta(T)-2}\frac{1}{2}\sum_{i=1}^{(k-\eta(t)+1)}\sum_{j=1}^{(a-\eta(t)+1)} \gamma_i\gamma_j\Phi(x_{\eta(t)-1},t)\{\Lambda^2(t,x_{k+1}) - \Lambda^2(t,x_k)\}$$

Therefore, the bond price is given by

$$
\begin{aligned}
B(t,T) &= \exp\Big(- \int_t^T f(t,u)du \Big) \\
&= \frac{B(0,T)}{B(0,t)} \exp\Big(- \sum_{b=0}^{\eta(t)-2} \Lambda_{x_{\eta(T)-1}}(x_{b+1},T) y_{\eta(T)-1}(x_{b+1}) \\
&- \Lambda_{x_{\eta(T)-1}}(t,T) y_{\eta(T)-1}(t) \\
&- \sum_{k=\eta(t)}^{\eta(T)-2} \sum_{b=0}^{\eta(t)-2} \Lambda_{x_k}(x_{b+1},x_{k+1}) y_k(x_{b+1}) \\
&- \sum_{k=\eta(t)}^{\eta(T)-2} \Lambda_{x_k}(t,x_{k+1}) y_k(t) \\
&- \frac{1}{2} \sum_{b=0}^{\eta(t)-2} \sum_{i=1}^{\eta(T)-1-b} \sum_{j=1}^{\eta(T)-1-b} \gamma_i \gamma_j \Phi(x_b,x_{b+1}) \{ \Lambda^2(x_{b+1},T) - \Lambda^2(x_{b+1},x_{\eta(T)-1}) \} \\
&- \frac{1}{2} \sum_{i=1}^{\eta(T)-\eta(t)} \sum_{j=1}^{\eta(T)-\eta(t)} \gamma_i \gamma_j \Phi(x_{\eta(t)-1},t) \{ \Lambda^2(t,T) - \Lambda^2(t,x_{\eta(T)-1}) \} \\
&- \sum_{k=\eta(t)}^{\eta(T)-2} \frac{1}{2} \sum_{b=0}^{\eta(t)-2} \sum_{i=1}^{k-b} \sum_{j=1}^{k-b} \gamma_i \gamma_j \Phi(x_b,x_{b+1}) \{ \Lambda^2(x_{b+1},x_{k+1}) - \Lambda^2(x_{b+1},x_k) \} \\
&- \sum_{k=\eta(t)}^{\eta(T)-2} \frac{1}{2} \sum_{i=1}^{(k-\eta(t)+1)} \sum_{j=1}^{(a-\eta(t)+1)} \gamma_i \gamma_j \Phi(x_{\eta(t)-1},t) \{ \Lambda^2(t,x_{k+1}) - \Lambda^2(t,x_k) \} \Big)
\end{aligned}
$$

Appendix B The impact of the futures price approximations in the Gaussian case

Futures	market price	start	end	Price with approx.	MC price	95% ci (2m paths)		Diff. (bp)
SLV20 (Oct '20)	99.9200	1/10/2020	31/10/2020	99.9220	99.9220	99.9220	99.9220	0.0000
SLX20 (Nov '20)	99.9250	1/11/2020	30/11/2020	99.9295	99.9296	99.9294	99.9297	0.0085
SLZ20 (Dec '20)	99.9250	1/12/2020	31/12/2020	99.9242	99.9241	99.9238	99.9243	-0.0133
SLF21 (Jan '21)	99.9150	1/01/2021	31/01/2021	99.9198	99.9199	99.9197	99.9202	0.0124
SLG21 (Feb '21)	99.9300	1/02/2021	28/02/2021	99.9320	99.9320	99.9316	99.9324	0.0000
SLH21 (Mar '21)	99.9350	1/03/2021	31/03/2021	99.9356	99.9352	99.9348	99.9356	-0.0373
SLJ21 (Apr '21)	99.9350	1/04/2021	30/04/2021	99.9393	99.9392	99.9388	99.9397	-0.0101
SLK21 (May '21)	99.9350	1/05/2021	31/05/2021	99.9300	99.9299	99.9294	99.9304	-0.0078
SLM21 (Jun '21)	99.9350	1/06/2021	30/06/2021	99.9347	99.9337	99.9331	99.9342	-0.0986
SLN21 (Jul '21)	99.9400	1/07/2021	31/07/2021	99.9400	99.9398	99.9391	99.9404	-0.0248
SLQ21 (Aug '21)	99.9450	1/08/2021	31/08/2021	99.9400	99.9392	99.9386	99.9399	-0.0778
SLU21 (Sep '21)	99.9400	1/09/2021	30/09/2021	99.9400	99.9397	99.9390	99.9404	-0.0301
SLV21 (Oct '21)	99.9400	1/10/2021	31/10/2021	99.9400	99.9389	99.9382	99.9397	-0.1067
Futures	market price	start	end	Price with approx.	MC price	95% ci (2m paths)		Diff. (bp)
SQU20 (Sep '20)	99.9275	16/09/2020	15/12/2020	99.9252	99.9253	99.9252	99.9254	0.0049
SQZ20 (Dec '20)	99.9300	16/12/2020	16/03/2021	99.9255	99.9251	99.9248	99.9255	-0.0367
SQH21 (Mar '21)	99.9350	17/03/2021	15/06/2021	99.9346	99.9344	99.9339	99.9348	-0.0280
SQM21 (Jun '21)	99.9350	16/06/2021	21/09/2021	99.9399	99.9390	99.9384	99.9397	-0.0857
SQU21 (Sep '21)	99.9350	15/09/2021	21/12/2021	99.9400	99.9380	99.9372	99.9388	-0.1991
SQZ21 (Dec '21)	99.9450	15/12/2021	15/03/2022	99.9500	99.9468	99.9459	99.9477	-0.3142
SQH22 (Mar '22)	99.9750	16/03/2022	21/06/2022	99.9704	99.9665	99.9655	99.9675	-0.3932
SQM22 (Jun '22)	99.9650	15/06/2022	20/09/2022	99.9700	99.9647	99.9636	99.9658	-0.5277

Table 3: Approximate vs. exact futures prices based on market conditions in September 2020.

This table compares three sets of futures prices, using the empirically fitted model parameters:

1. Market prices observed in September 2020,
2. the "calibrated prices" of the futures contracts used in our analysis, i.e., the prices calculated under the approximations (47) and (48),
3. and the corresponding prices calculated without making these assumptions (using Monte Carlo simulation).

As the final column of the table shows, the impact of the approximations (47) and (48) is negligible, i.e., the difference between the prices calculated under these approximations and the Monte Carlo estimate of the exact model price is well less than one basis point in all cases.

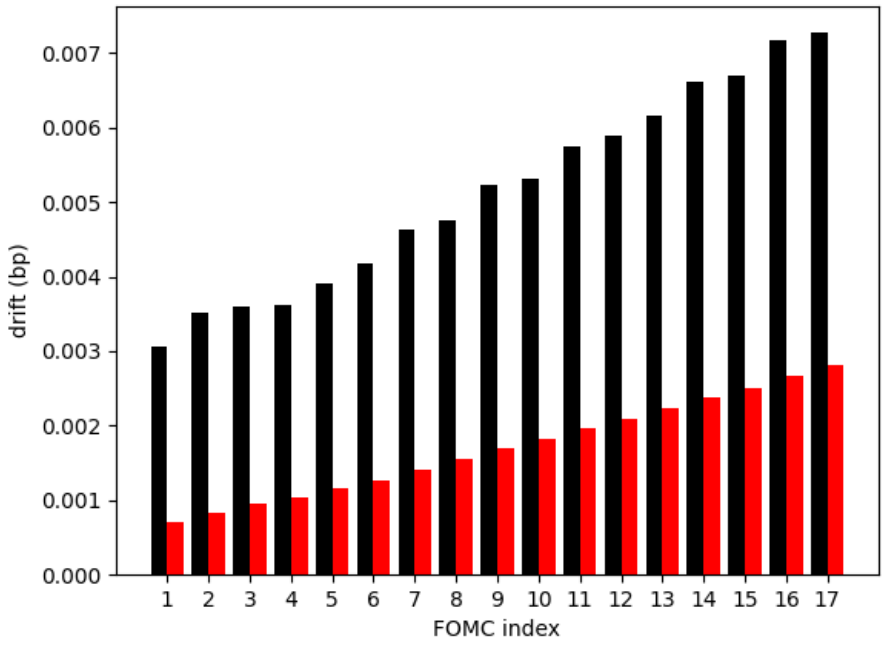

Figure 19: average daily drift adjustment for $t = 3$ (black) and $t = 1.5$ (red)

Appendix C The impact of the risk–neutral HJM drift term

In this section we use the results obtained using the calibration results, Eq. (61) and Eq. (66) to calculate the drift component of the Gaussian version of the model as shown in Eq. (4). We demonstrate that including the drift would have a negligible impact on the state estimates as well as the RMSE results.

The first step is to estimate σ_j from the realised variance of the factor states shown in Fig. **??**. The estimated σ_j is then used to calculate the drift component in Eq. (61) for various values of t and T in a three–factor model.

The results focus on the time periods for the data used in this paper ($t = 3$ and $T = 2$) as well as Skov and Skovmand (2021) ($t = 1.5$ and $T = 2$). The average daily drift adjustment is shown in Fig. 19 as a function of the distance between t and T measured in the number of FOMC meetings. The drift adjustment at most amounts to less than 0.01 basis points per day. This is well below the 0.25 basis point minimum tick bid/ask spread of the futures. If the estimated states were adjusted for the drift, this amount would have a negligible impact on the daily increments shown in Fig. 19 and therefore would not change the σ_j estimate.

The drift adjustment term structure at the end of each observation period is shown in Fig. 20. Unsurprisingly, the risk–neutral drift term structure is piecewise constant in T. The term structure does suggest that over time the drift adjustment accumulates to a significant amount, enough to impact the RMSE results. However, although there is some gradient in the sections between FOMC meetings, the shape of the term structure is dominated by the increases on FOMC meeting dates. Therefore the daily adjustments, which as argued would not impact the state estimates, would remove most of the accumulated drift leaving only the negligible gradient in between FOMC meetings.

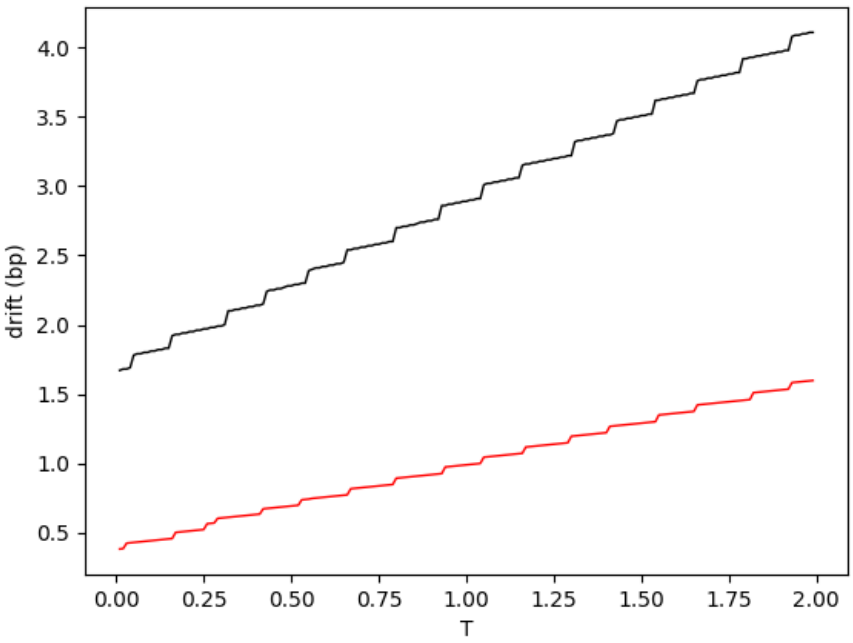

Figure 20: drift termstructure for $t = 3$(black) and $t = 1.5$

References

Alfeus, M., Grasselli, M. and Schlögl, E.: 2020, A Consistent Stochastic Model of the Term Structure of Interest Rates for Multiple Tenors, *Journal of Economic Dynamics and Control* **114**.

Andersen, L. B. G. and Bang, D. R. A.: 2020, Spike Modelling for Interest Rate Derivatives with an Application to SOFR Caplets. Available at SSRN: https://papers.ssrn.com/sol3/papers.cfm?abstract_id=3700446.

Backwell, A. and Hayes, J.: 2022, Expected and unexpected jumps in the overnight rate: consistent management of the libor transition, *Journal of Banking & Finance* p. 106669.

Backwell, A., Macrina, A., Schlögl, E. and Skovmand, D.: 2023, Term rates, multicurve term structures and overnight rate benchmarks: A roll-over risk approach, *Frontiers of Mathematical Finance* .

Binder, A. S.: 2010, Quantitative Easing: Entrance and Exit Strategies, *Federal Reserve Bank of St. Louis Review* **92**(6), 465–79.

Brace, A., Gatarek, D. and Musiela, M.: 1997, The Market Model of Interest Rate Dynamics, *Mathematical Finance* **7**(2), 127–155.

Cox, J. C., Ingersoll, J. E. and Ross, S. A.: 1981, The relation between forward prices and futures prices, *Journal of Financial Economics* **9**, 321–346.

Cox, J. C., Ingersoll, J. E. and Ross, S. A.: 1985, A Theory of the Term Structure of Interest Rates, *Econometrica* **53**(2), 385–407.

Federal Open Market Committee: 2000-2020, Minutes of the Federal Open Market Committee.

Fontana, C., Grbac, Z., Gümbel, S. and Schmidt, T.: 2020, Term Structure Modelling for Multiple Curves with Stochastic Discontinuities, *Finance and Stochastics* **24**(2), 465–511.

Gellert, K. and Schlögl, E.: 2021, Short Rate Dynamics: A Fed Funds and SOFR perspective, *Technical Report Available at SSRN: https://papers.ssrn.com/sol3/papers.cfm?abstract_id=3763589*, SSRN Working Paper.

Grzelak, L., Oosterlie, C. W. and Weeran, S. V.: 2008, Extension of stochastic volatility equity models with the hull white interest rate process, *Quantitative Finance* **12**(1).

Hagan, P. S., Kumar, D., Lesniewski, A. S. and Woodward, D. E.: 2002, Managing smile risk, *The Best of Wilmott* **1**, 249–296.

Heath, D., Jarrow, R. and Morton, A.: 1992, Bond Pricing and the Term Structure of Interest Rates: A New Methodology for Contingent Claims Valuation, *Econometrica* **60**(1), 77–105.

Heitfield, E. and Park, Y.-H.: 2019, Inferring Term Rates from SOFR Futures Prices. Available at SSRN: https://papers.ssrn.com/sol3/papers.cfm?abstract_id=3352598.

Heston, S.: 1993, A closed–form solution for options with stochastic volatility, with application to bond and currency options, *The Review of Financial Studies* **6**, 327–343.

Hilton, S.: 2005, Trends in Federal Funds Rate Volatility, Federal Reserve Bank of New York, *Current Issues in Economics and Finance* **11**(7).

Hull, J. and White, A.: 1990, Pricing Interest–Rate Derivative Securities, *Review of Financial Studies* **3**(4), 573–592.

Karlsson, P., Pilz, K. and Schlögl, E.: 2017, Calibrating a market model with stochastic volatility to commodity and interest rate risk, *Quantitative Finance* **17**(6).

Keller-Ressel, M., Schmidt, T. and Wardenga, R.: 2018, Affine Processes Beyond Stochastic Continuity, *Annals of Applied Probability* **29**(6), 3387–3437.

Kim, D. H. and Wright, J. H.: 2014, Jumps in Bond Yields at Known Times, *National Bureau of Economic Research* (No. w20711).

Lyashenko, A. and Mercurio, F.: 2019, Looking Forward to Backward-Looking Rates: A Modeling Framework for Term Rates Replacing LIBOR. Available at SSRN: https://ssrn.com/abstract=3330240.

Mercurio, F.: 2018, A Simple Multi-Curve Model for Pricing SOFR Futures and Other Derivatives. Available at SSRN: https://ssrn.com/abstract=3225872.

Merton, R. C.: 1973, Theory of Rational Option Pricing, *Bell Journal of Economics and Management Science* pp. 141–183.

Miltersen, K. R., Sandmann, K. and Sondermann, D.: 1997, Closed Form Solutions for Term Structure Derivatives with Log-Normal Interest Rates, *The Journal of Finance* **52**(1), 409–430.

Musiela, M. and Rutkowski, M.: 1997, Continuous–Time Term Structure Models: A Forward Measure Approach, *Finance and Stochastics* **1**(4).

Nelson, C. R. and Siegel, A. F.: 1987, Parsimonious Modeling of Yield Curves, *The Journal of Business* **60**(4), 473–489.

Piterbarg, V.: 2015, *A stochastic volatility forward Libor model with a term structure of volatility smiles.* Available at SSRN: https://ssrn.com/abstract=359001.

Schlögl, E., Skov, J. B. and Skovmand, D.: 2023, Term Structure Modeling of SOFR: Evaluating the Importance of Scheduled Jumps. Available at SSRN: https://papers.ssrn.com/sol3/papers.cfm?abstract_id=4431839.

Schrimpf, A. and Sushko, V.: 2019, Beyond LIBOR: A Primer on the New Reference Rates, *BIS Quarterly Review* .

Skov, J. B. and Skovmand, D.: 2021, Dynamic Term Structure Models for SOFR Futures, *Journal of Futures Markets* **41**(10).

The Alternative Reference Rates Committee: 2018, Second Report.

Vasicek, O.: 1977, An Equilibrium Characterization Of The Term Structure, *Journal Of Financial Economics* **5**(2), 177–188.

Data availability statement

Market data (history of closing futures prices) was obtained from Barchart and are available at `https://www.barchart.com`. Economic data was obtained from Federal Reserve New York and Federal Reserve Bank of St. Louis online databases, see `https://www.newyorkfed.org/data-and-statistics` and `http://fred.stlouisfed.org`.